

1 **Can Prediction Error Explain Predictability Effects on the N1 during**
2 **Picture-Word Verification?**


3 Jack E. Taylor^{1,2}, Guillaume A. Rousselet², and Sara C. Sereno²

4 ¹Department of Psychology, Goethe University Frankfurt

5 ²School of Psychology and Neuroscience, University of Glasgow

6 **Author Note**

7
8 Jack E. Taylor  <https://orcid.org/0000-0003-4765-0118>

9 Guillaume A. Rousselet  <https://orcid.org/0000-0003-0006-8729>

10 Sara C. Sereno  <https://orcid.org/0000-0001-7957-9542>

11 Correspondence concerning this article should be addressed to Jack E. Taylor
12 Department of Psychology, Goethe University Frankfurt; E-mail:
13 Taylor@psych.uni-frankfurt.de

Abstract

14

15 Do early effects of predictability in visual word recognition reflect prediction error?

16 Electrophysiological research investigating word processing has demonstrated predictability
17 effects in the N1, or first negative component of the event-related potential (ERP).

18 However, findings regarding the magnitude of effects and potential interactions of

19 predictability with lexical variables have been inconsistent. Moreover, past studies have

20 typically used categorical designs with relatively small samples and relied on by-participant

21 analyses. Nevertheless, reports have generally shown that predicted words elicit less

22 negative-going (i.e., lower amplitude) N1s, a pattern consistent with a simple predictive

23 coding account. In our preregistered study, we tested this account via the interaction

24 between prediction magnitude and certainty. A picture-word verification paradigm was

25 implemented in which pictures were followed by tightly matched picture-congruent or

26 picture-incongruent written nouns. The predictability of target (picture-congruent) nouns

27 was manipulated continuously based on norms of association between a picture and its

28 name. ERPs from 68 participants revealed a pattern of effects opposite to that expected

29 under a simple predictive coding framework.

30 *Keywords:* N1, N170, Prediction, Predictive Coding, Word Recognition

Can Prediction Error Explain Predictability Effects on the N1 during Picture-Word Verification?

Introduction

Readers and listeners routinely use context to predict upcoming semantic and lexical content. Evidence for such predictive processes arises from both behavioural and neural correlates of language comprehension (Kuperberg & Jaeger, 2016; Luke & Christianson, 2016; Pickering & Gambi, 2018; Rayner et al., 2011; Van Petten & Luka, 2012), with demonstrated facilitation for the processing of predicted information (Federmeier, 2007; Pickering & Garrod, 2013).

A key question in this area is, how early in the processing stream are predictive processes able to modulate visual word recognition? One early stage in visual word recognition which may be sensitive to prediction involves the processing of visual word forms. A word form can be defined as the visual pattern of a single written word, comprised of smaller orthographic components (e.g., letters, letter bigrams, graphemes, strokes). While some electrophysiological evidence suggests sensitivity to orthographic variables in an earlier posterior P1 component peaking at around 100 ms after word presentation (e.g., Nobre et al., 1994; Segalowitz & Zheng, 2009; Sereno et al., 1998), the event-related potential (ERP) component most identified as an index of orthographic processing across different scripts is the first posterior negative-going wave, the N1 (Bentin et al., 1999; Lin et al., 2011; Ling et al., 2019; Maurer, Brandeis, et al., 2005; Maurer et al., 2008; Pleisch et al., 2019). The N1 is also sometimes referred to as the N170 due to the timing of its peak in some studies, at around 170 ms. This typically occipitotemporal, negative-going component shows reliable differences between orthographic and non-orthographic stimuli (e.g., words elicit more negative-going N1s than false-font strings do; Appelbaum et al., 2009; Bentin et al., 1999; Eberhard-Moscicka et al., 2016; Maurer, Brandeis, et al., 2005; Maurer, Brem, et al., 2005; Pleisch et al., 2019; Zhao et al., 2014).

Accounts of orthographic processing often stress the importance of top-down

58 predictions, and their interactions with bottom-up sensory input. For instance, the
59 interactive account of the ventral occipito-temporal cortex (vOT), a region which is a likely
60 generator of the N1 ERP component (Allison et al., 1994; Brem et al., 2009; Cohen et al.,
61 2000; Dale et al., 2000; Maurer, Brem, et al., 2005; Nobre et al., 1994; Taha et al., 2013;
62 Woolnough et al., 2021), suggests that sensitivity to orthography arises through the
63 synthesis of bottom-up visuospatial information and top-down predictions informed by
64 prior experience and knowledge (Price & Devlin, 2011). Such accounts exist within a
65 predictive coding framework, according to which the brain utilises higher-level information
66 to build, maintain, and continually update a generative model (or hierarchical series of
67 generative models) of sensory information (Friston, 2010; Rao & Ballard, 1999; Rauss
68 et al., 2011). A key feature of such accounts is that higher-level predictions cause
69 lower-level features to be preactivated, and that the difference between the bottom-up
70 sensory input and top-down predictions corresponds to a prediction error, which the brain
71 attempts to minimise (Clark, 2013; Walsh et al., 2020).

72 In a predictive coding framework, prediction errors are determined by two key
73 attributes: the magnitude of the error, and the precision or certainty of the error (Feldman
74 & Friston, 2010; Kanai et al., 2015). Feldman and Friston (2010) likened the error signal to
75 the calculation of the t statistic, where magnitude of an observation (i.e., mean, or mean
76 difference) is divided by the inverse of its precision (i.e., standard error). Prediction errors,
77 weighted by precision in this manner, can be conceptualised as representing the degree of
78 “surprise” associated with a set of observations under a specified hypothesis.

79 Firstly, the magnitude of the error should determine the size of the error signal, with
80 larger prediction errors resulting from greater mismatch between descending (top-down)
81 predictions and ascending (bottom-up) sensory input. In neutral (non-biasing) contexts, a
82 predictive coding account that includes learning of statistical regularities over extended
83 periods would assert that error signals should vary as a function of stimulus regularity.
84 More specifically, a predictive coding account of orthographic processing would expect error

85 signals to vary as a function of the size of the difference between a general orthographic
86 prior (e.g., an average word form) and a presented word form. Some recent findings appear
87 to support the notion that the N1 reflects a neutral-context error signal, with greater
88 distance from an orthographic prior eliciting greater amplitude (Gagl et al., 2020), while
89 the profile of the N1's sensitivity to word form regularity over experience matches that
90 expected under a predictive coding account (Huang et al., 2022; Zhao et al., 2019).

91 Secondly, the precision or certainty of the prediction error should influence the
92 response, with more certain descending predictions, and more certain ascending sensory
93 input, eliciting greater error signals when predictions are violated. In neutral contexts,
94 predictions, and certainty about them, may not be expected to vary much from a
95 context-general prior. Indeed, it is easier to envisage the expected role of prediction
96 precision for orthographic processing in biasing contexts, where precision is more variable
97 than it is in neutral contexts. A predictive coding model of orthographic processing that
98 allows for online, context-informed updating of orthographic priors would expect that the
99 predictability of word forms should influence error responses, with more predictable
100 contexts eliciting stronger error signals when word forms are prediction-incongruent, and
101 weaker error signals when prediction-congruent. For instance, a sentential context that
102 elicits a clear and reliable prediction for an upcoming word (i.e., that has high Cloze
103 probability) should show a larger prediction error difference, between succeeding
104 prediction-congruent and -incongruent word forms, than should a more neutral sentential
105 context that is consistent with a large number of low-probability candidate words.

106 In this paper, we examine whether a simple predictive coding account that includes
107 online updating of context-biased predictions and expectations can explain neural activity,
108 captured in the N1, elicited by a word in context. Specifically, we examine whether
109 sensitivity to prediction error in the N1 is dependent on contextual predictability, as a
110 predictive coding account would expect. We hypothesise that according to a simple
111 predictive coding model, the N1 should be larger for prediction-incongruent than

112 prediction-congruent word forms, in a manner dependent on the level of predictability, with
113 greater differences at higher levels of predictability. Studies examining the effect of
114 predictability on the N1's amplitude and latency have principally manipulated readers'
115 expectations for specific visual word forms. Here, expectations are typically biased via
116 linguistic contexts, where an initial text varies in how predictable it makes an upcoming
117 target word form. In an alternative approach, bias is achieved via non-linguistic cues, such
118 as cross-modal contexts and manipulation of task demands.

119 **Biasing Word Form Predictions via Linguistic Cues**

120 Readers' predictions of upcoming word forms are generally manipulated via
121 linguistic cues. In these studies, a target word's predictability is typically determined in a
122 pre-experiment norming study, operationalised via Cloze probability (i.e., the probability
123 that the target is correctly guessed given its preceding context). Such a measure of word
124 form predictability aligns closely with the concept of prediction precision or certainty in a
125 predictive coding account.

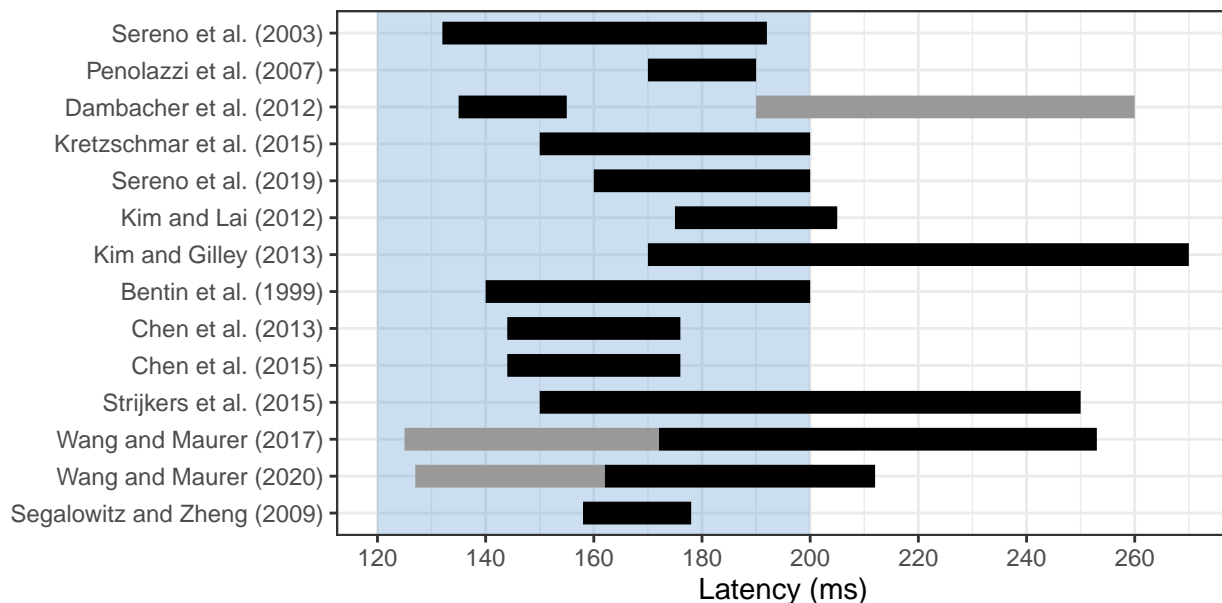
126 Recent ERP investigations that have manipulated sentential context have also often
127 varied word frequency, with the assumption that an interaction of predictability with word
128 frequency would provide evidence for top-down influences on lexical access. Such studies
129 have demonstrated effects in the N1, although the pattern of effects observed across studies
130 is varied (for a review, see Sereno et al., 2019). While effects often extend to earlier and
131 later components, we limit our discussion to those involving predictability within the N1
132 window. Except where noted, electrodes analysed for the N1 were located
133 occipitotemporally, and sentences were displayed word-by-word, using different word
134 presentation rates or stimulus onset asynchronies (SOAs). It is important to note that the
135 designated 'N1' time window differs across studies, as illustrated in Figure 1. Our review of
136 studies utilising sentential contexts is presented chronologically. Sereno et al. (2003), using
137 a 450 ms SOA, manipulated predictability (low, high) and word frequency (low, high), and
138 found an interaction of these factors in the N1 (132-192 ms) across posterior and anterior

139 sites (comprising their first factor in a spatial factor analysis). Their predictability effect
140 demonstrated less negative amplitudes at higher predictability, but only for low (and not
141 high) frequency words. In a similar study, but using a 700 ms SOA, Penolazzi et al. (2007)
142 manipulated predictability (low, high), word frequency (low, high), and, additionally, word
143 length (monosyllabic words with an average of 4.08 letters, vs. disyllabic words with an
144 average of 6.25 letters). In a 170-190 ms window, they found that high predictability
145 conditions showed a more negative-going amplitude over centroparietal sites than low
146 predictability conditions, but, unlike Sereno et al. (2003), found no interaction with word
147 frequency. In addition, no significant interaction was observed with length. In a German
148 study, Dambacher et al. (2012) varied predictability (low, high) and word frequency (low,
149 high) in three experiments using different SOAs. At the shortest SOA of 280 ms, but not
150 at SOAs of 490 or 700 ms, they found an interaction of predictability and frequency in the
151 early portion of the N1 (135-155 ms). For high predictable words only, there was a
152 frequency effect, with low frequency words showing a more negative-going amplitude than
153 high frequency words over posterior sites. In a later N1 window, from 190 to 260 ms,
154 Dambacher et al. reported an effect of frequency, but no interaction with (or main effect
155 of) predictability. In a study measuring both eye movements and EEG during normal
156 reading, Kretzschmar et al. (2015) manipulated items' predictability (low, high) and
157 frequency (low, high). Testing only bilateral centroparietal electrodes, their fixation-related
158 potentials (FRPs) demonstrated a main effect of predictability in a 150-200 ms window,
159 with high predictable words showing a more positive-going amplitude than low predictable
160 words, but without any interaction with frequency. Finally, Sereno et al. (2019)
161 manipulated both predictability (low, high) and frequency (low, high). While the first,
162 context sentence was presented in full, the second sentence containing the target word was
163 presented word-by-word, with a short, 300 ms SOA. Sereno et al. (2019) found a
164 predictability-frequency interaction in the N1 (160-200 ms). A predictability effect emerged
165 only for high frequency words. Amplitudes to low predictable words, in comparison to those

166 to high predictable words, were more positive-going over left-hemisphere sites, but more
167 negative-going over right-hemisphere sites. In sum, while these studies using sentential
168 contexts have reported predictability effects in the N1 window, it is clear that the timing
169 and topography of effects, as well as interactions with frequency, have been inconsistent.

Figure 1

N1 windows in predictability studies.



Some studies analysed two N1 windows (e.g., onset and offset). N1 windows reported to show a predictability effect are highlighted in black, while N1 windows that failed to show a predictability effect are highlighted in grey. Studies are listed in order of their mention in our review. For reference, the blue region displays the N1 period that we pre-registered.

170 Instead of manipulating error precision or certainty as the above studies have by
171 varying predictability, A. Kim and Lai (2012) manipulated the orthographic error
172 magnitude. Using a 550 ms SOA, the target word or alternative orthographic versions of it
173 were presented in contexts that were acutely predictive of the target ($M_{Cloze}=.90$).
174 Contexts were followed by the predictable target word (e.g., *cake*), an orthographically
175 similar pseudoword (e.g., *ceke*), an orthographically dissimilar pseudoword (e.g., *tont*), or a
176 consonant-string nonword (e.g., *srdt*). Consistent with an orthographic explanation for
177 prediction effects in the N1, relative to targets, N1 (175-205 ms) amplitude was more

178 negative-going for orthographically dissimilar pseudowords and nonwords (i.e., when
179 orthographic prediction error magnitude was greater). Orthographically similar
180 pseudowords, while significantly different from all other conditions in the earlier P1,
181 elicited N1 components more similar in amplitude to target words.

182 Another linguistic cue that has been manipulated is grammaticality. A. E. Kim and
183 Gilley (2013) demonstrated effects of syntactic anomaly on the N1. Sentences leading to a
184 strong prediction for the determiner, *the*, were presented unchanged or with the determiner
185 replaced with an agrammatic preposition (e.g., *The thief was caught by the/for police*). The
186 left-lateralised occipitotemporal N1 (170-270 ms) was more negative-going with the
187 syntactically anomalous preposition than with the determiner. As the authors point out,
188 the N1 effect is unlikely to be evidence for sensitivity to syntax per se. Rather, given
189 evidence of the N1's sensitivity to orthographic features, it is probably more accurate to
190 posit that the high predictability of the determiner's orthographic features elicited a less
191 negative-going N1 when these predictions were confirmed.

192 A. E. Kim and Gilley (2013) simultaneous manipulation of orthography and syntax
193 highlights a prevalent issue within the literature: namely, altering the visual word form
194 necessitates alteration of the semantics, syntax, and/or plausibility of the sentence or wider
195 discourse. Another limitation shared by studies using word-by-word presentation of
196 sentences is that ERPs elicited by the target word can become difficult to disentangle from
197 ERPs elicited by preceding or succeeding words, especially if the SOA is short or
198 unjittered. While fast presentation times of sentential contexts and targets are useful for
199 demonstrating that early modulation by predictive processes extends to realistic reading
200 rates, their application may not be necessary to demonstrate that such modulation can
201 occur. It is also of note that in a recent review of ERP studies using sentence- and
202 discourse-level contexts to examine early neural correlates of word form prediction,
203 Nieuwland (2019) concluded that findings thus far have been weak, inconsistent, and in
204 need of more replication attempts. Moreover, most studies to date were not pre-registered

205 and often used inappropriate analysis models that did not account for measurement
206 variability, raising questions about false positives in that literature.

207 **Biasing Word Forms via Non-Linguistic Cues**

208 Effects of prediction and expectation may alternatively be investigated using
209 paradigms that modulate non-linguistic features of tasks and stimuli. In one approach,
210 identical or suitably matched stimuli are presented under different task instructions (e.g.,
211 Compton et al., 1991). For instance, participants are more likely to predict and show
212 sensitivity to lexical variables if given a word-nonword task than one which requires
213 judgements on a non-lexical dimension, such as font colour. In a French study, Bentin et al.
214 (1999) presented words, pseudowords, and consonant strings in a series of different tasks
215 requiring participants to mentally count the word targets (oddballs) among word and
216 nonword distractors. The tasks included lexical decision (word vs. nonword), semantic
217 categorisation (i.e., abstract vs. concrete words or nonwords), and rhyme judgement (i.e.,
218 rhymes vs. does not rhyme with "-ail"). Although plots of ERPs and topographies suggest
219 a trend towards a task-stimulus-hemisphere interaction on the N1 (140-200 ms), with the
220 difference between orthographically plausible and implausible stimuli being larger in the
221 tasks requiring lexical or semantic processing than in the rhyme task, the effect of task was
222 not tested as a factor, such that any task-stimulus interaction is very difficult to interpret.
223 Chen et al. (2013) compared ERP responses to target words in lexical decision and
224 semantic categorisation (i.e., word vs. person's name) tasks to a condition with minimal
225 task demands, namely silent word reading. They identified an effect of task on the N1
226 (144-176 ms), with a more negative-going N1 for words observed in lexical decision and
227 semantic categorisation than in silent word reading. In a similar study, Chen et al. (2015)
228 further suggested that the degree to which variables like frequency and imageability affect
229 activity in the N1 (144-176 ms) was task-dependent. For instance, Chen et al. (2015)
230 showed that increases in word frequency were associated with decreases in source-space
231 activity during the N1, and that, crucially, this effect was larger in lexical decision than in

232 semantic decision (i.e., word vs. person's name) or silent word reading. In a French study
233 examining word frequency effects across different go/no-go tasks, Strijkers et al. (2015)
234 similarly reported that ERP amplitude in a period including the N1 (150-250 ms) was
235 more sensitive to word frequency (with more negative amplitudes for higher frequency
236 words) during a semantic categorisation (i.e., animal vs. non-animal) than a colour
237 categorisation (i.e., blue vs. non-blue) task. Wang and Maurer (2017) applied a similar
238 paradigm to examine how task modulated the effect of script familiarity on the N1
239 (125-253 ms) ERP. Chinese-reading participants were presented on each trial with either
240 familiar Chinese characters or stroke-matched, unfamiliar Korean symbols, in three tasks:
241 repetition detection, colour categorisation, and delayed naming (where participants would
242 respond "symbol" to Korean characters). Wang and Maurer (2017) showed that the N1's
243 sensitivity to character familiarity (with more negative amplitudes for unfamiliar Korean
244 symbols than familiar Chinese characters) was greater in delayed naming and colour
245 categorisation tasks than in a repetition detection task. This effect was specifically
246 observed in the N1's offset period of 172-253 ms, where onsets and offsets are defined
247 respectively as the periods in the component's time window which precede and succeed its
248 peak. That the effect of character familiarity differed between colour categorisation and
249 repetition detection is not straightforward to interpret, as these tasks may be expected to
250 require similarly shallow processing of orthography. Nevertheless, the difference between
251 delayed naming (which necessitates orthographic processing) and repetition detection
252 (which does not) is suggestive of an effect of task demands on sensitivity to orthographic
253 familiarity. Related non-sentential approaches to biasing participants' word form
254 predictions include an attempt to alter expectations for different types of script. Wang and
255 Maurer (2020) found that native Mandarin speakers' N1 sensitivity (onset 127-162 ms;
256 offset 162-212 ms) to character familiarity, where unfamiliar Korean characters elicit
257 greater N1 offset amplitudes than familiar Chinese characters, was greater when
258 participants were led to expect Chinese characters.

259 In addition to task manipulations, non-sentential semantic contexts, leading to
260 predictions for specific words or categories of words, have also been used to investigate
261 predictive processing. In an ERP study, Segalowitz and Zheng (2009) presented words and
262 pseudowords for lexical decisions in two conditions: words were either drawn from a single
263 category (e.g., animals), or from five different semantic categories. Segalowitz and Zheng
264 reported an interaction between stimulus type (word vs. pseudoword) and expectation (one
265 vs. five categories) in the N1 (158-178 ms), wherein expectation affected N1 amplitudes for
266 words but not for pseudowords. Their finding suggested that the N1 was sensitive to the
267 greater predictive strength of a single semantic category. Using a similar paradigm, Hauk
268 et al. (2012) compared ERPs in lexical (word vs. pseudoword) and semantic (living vs.
269 non-living) decision tasks, showing that effects of category relevance were observed in the
270 semantic decision task as early as 166 ms (data were analysed continuously, with no N1
271 window definition). This finding suggests, consistent with the findings of Segalowitz and
272 Zheng, an early sensitivity to category relevance during the N1 which, given the N1's
273 robust sensitivity to orthography, is likely to reflect an influence of semantic-level
274 predictions on orthographic processing.

275 In another attempt to modulate top-down expectancy without linguistic context,
276 Dikker and Pyllkanen (2011) implemented a picture-noun phrase verification task. An
277 image of a target object alone or an image of objects related to the target object was
278 followed by a written noun phrase (article + noun) denoting the target object. They
279 manipulated congruency and predictability. For congruent trials, the noun phrase referred
280 to a food/drink or animal (e.g., *the apple* or *the monkey*) that matched the prior image of
281 the object presented on its own or 'contained' in a stylized image (e.g., a grocery bag or
282 Noah's Ark, respectively). In the incongruent condition, the noun phrase did not match
283 the prior image (single object or collection of objects). Predictability was considered high
284 when the target object appeared on its own, and was considered low when the target object
285 could be inferred to exist within the stylized images. Example conditions for the noun

286 phrase, *the apple*, are determined by its preceding image as follows: an apple (congruent,
287 high predictability), a banana (incongruent, high predictability), a bag of groceries
288 (congruent, low predictability), or Noah's Ark (incongruent, low predictability). Noun
289 phrases (40 food/drink, 40 animal) were repeated four times across conditions. Although
290 Dikker and Pyllkanen did not examine effects in the MEG equivalent of an N1 window,
291 they did find effects of congruency only in the high predictive condition (i.e., the apple
292 preceded by an apple vs. a banana image) in temporal windows preceding (~100 ms) and
293 succeeding (250-400 ms) the N1. Their stimuli were designed to minimise orthographic
294 similarity between congruent and incongruent pairs of noun phrases (i.e., maximising the
295 magnitude of orthographic errors), suggesting that the authors anticipated that any early
296 sensory effect of predictability may be related to orthographic processing. With only 7
297 participants, the study likely lacked the sample size necessary to identify such an effect in
298 an N1-like window. Indeed, in a related paradigm using fMRI, Kherif et al. (2011)
299 presented picture and word prime-target pairs under four conditions: conceptual identity,
300 semantically related, shared initial phoneme, and unrelated. In addition, the prime was
301 either masked (after 33 ms) or not. The stimulus types of prime-target pairs were either
302 matching (word-word with varying typography, or picture-picture with different views) or
303 non-matching (word-picture or picture-word). In the unmasked conceptual identity
304 condition, Kherif et al. showed priming effects in the left vOT (likely generator for the N1)
305 for matching and non-matching stimulus types. Specifically, they showed that targets
306 elicited reduced left vOT activity if preceded by congruent primes, regardless of whether
307 the stimulus types were of matching or non-matching stimulus types. Assuming that
308 picture identity is not directly processed in the left vOT, these findings suggest that
309 higher-level processes link the identity and content of pictures to orthographic
310 representations of word forms. However, Kherif et al.'s use of fMRI prevents interpretation
311 of the timing of such effects - its coarse temporal resolution means that mapping of picture
312 content to representations in vOT could occur so late as to be irrelevant to initial

313 orthographic word recognition processes.

314 One advantage of paradigms like picture-word verification tasks is that the
315 researcher can control and manipulate variables like predictability and specificity of the
316 picture-word relation. This was demonstrated in the design used by Dikker and Pyllkanen
317 (2011), where the picture preceding the target word unambiguously biased participants'
318 expectations to a single word form (with an image of one clearly identifiable object), or
319 instead biased a set of semantically related possible word forms (with an image inducing
320 multiple object candidates). Such a manipulation is comparable to the use of Cloze
321 probability in sentential contexts or single versus multiple category priming, and similarly
322 aligns with the concept of error precision or certainty.

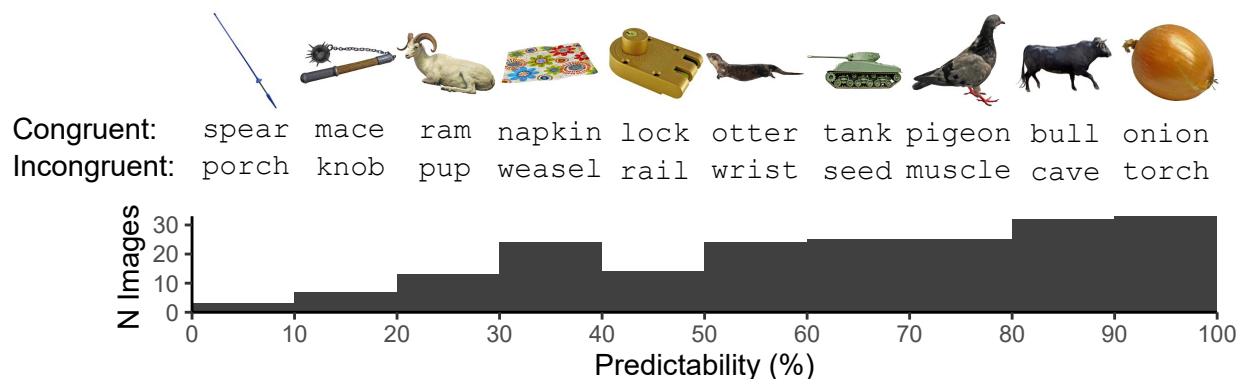
323 **The Present Study**

324 In the present study, we adapted the picture-word verification paradigm to examine
325 the role of Predictability in prediction effects on the N1. We presented participants with
326 PICTURE-word pairs that were congruent (e.g., ONION-onion) or incongruent (e.g.,
327 ONION-torch). Predictability of the congruent word was a continuous variable, dependent
328 upon how often the noun is reliably used in naming the picture (**Figure 2**). By
329 manipulating both Congruency and Predictability of word forms, we were able to examine
330 whether the effect of Congruency on the N1 (sensitivity to prediction error) is contingent
331 on Predictability (certainty or precision of prediction errors), in the manner expected
332 according to a simple predictive coding account of the N1 in which observed N1 magnitude
333 indexes prediction error.

334 We hypothesised, consistent with such a predictive coding account, that that there
335 would be a Congruency-Predictability interaction in which at the highest levels of
336 Predictability, N1s elicited by picture-incongruent words would be more negative-going
337 than those elicited by picture-congruent words, while at the lowest level of Predictability
338 picture-congruent and -incongruent words should elicit N1s of similar magnitude. We
339 anticipated three patterns of results that would have been consistent with this hypothesis:

Figure 2

Illustration of the experimental stimuli.



PICTURE-word pairs were either congruent (e.g., NAPKIN-*napkin*) or incongruent (e.g., NAPKIN-*weasel*), while predictability of congruent picture-word pairs varied continuously. Ten example picture-congruent and -incongruent pairs are presented, with their predictability corresponding to the histogram bin they appear above.

- 340 (1) higher levels of Predictability lead to a reduction in N1 magnitude only for
341 picture-congruent words, with no such effect for picture-incongruent words (**Figure 3a**);
- 342 (2) higher levels of Predictability lead to an increase in N1 magnitude only for
343 picture-incongruent words, with no such effect for picture-congruent words (**Figure 3b**); or
- 344 (3) higher levels of Predictability lead to both a reduction in N1 magnitude for
345 picture-congruent words and an increase in N1 magnitude for picture-incongruent words
346 (**Figure 3c**).

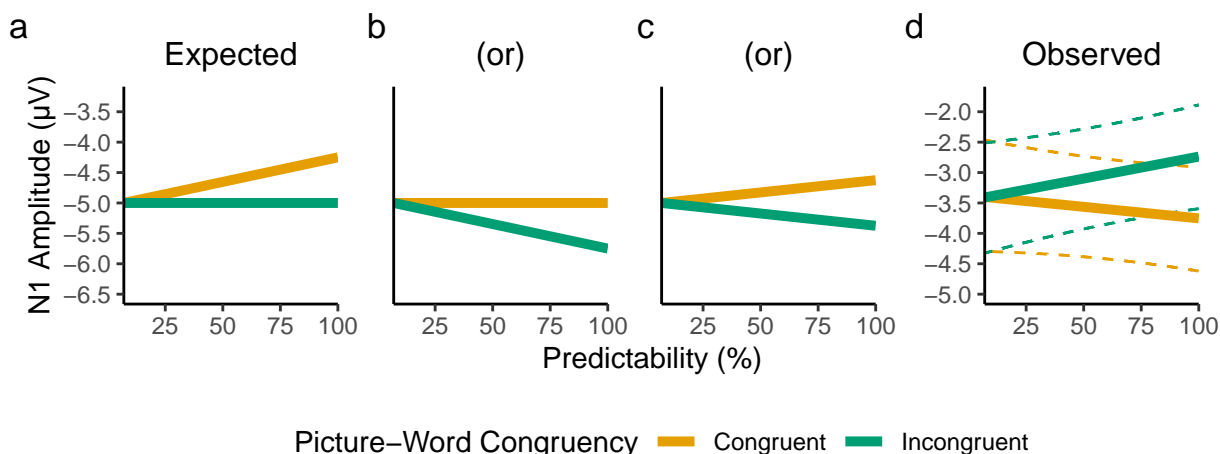
347 In our power analysis, we focused on the first of these possible patterns of results,
348 but importantly, the Congruency-Predictability interaction term that we pre-registered to
349 test our hypothesis (<https://osf.io/jk3r4>) would capture any of these patterns, as the
350 interaction term's coefficient would be in the same direction in all cases.

351 In our analysis, we found a pattern of effects counter to our pre-registered hypothesis
352 (**Figure 3d**), with a Congruency-Predictability interaction in the opposite direction. An
353 exploratory Bayesian analysis revealed that the observed interaction was 59.98 times more
354 likely than our hypothesis. Based on these findings, we argue our results suggest that such
355 a simplistic predictive coding account is, at least on its own, insufficient to explain the

356 pattern of prediction effects observed in the N1 during a picture-word verification task.

Figure 3

A comparison between the predicted (a,b,c) and observed (d) patterns of results.



The predicted pattern of results was based on a predictive coding interpretation of the N1, according to which the magnitude of the N1 should be smaller for picture-congruent words relative to picture-incongruent words, and to a greater extent as Predictability increases. The observed pattern of results depicts the fixed effect predictions from the pre-registered linear mixed-effects model, with dashed lines depicting 95% bootstrapped prediction intervals (estimated from 5,000 bootstrap samples).

357 This study was pre-registered at <https://osf.io/jk3r4> and the reported methodology
358 and planned analysis conform to that specified in the pre-registration, except for two
359 changes: an accidental change to timing of stimuli, and a lowering of the EEG high-pass
360 filter cut-off. We explain these changes in the relevant sections, and demonstrate in
361 **Supplementary Materials F** that the change to the high-pass filter cut-off had minimal
362 effect on the results and conclusions. All data and code are available at
363 <https://osf.io/389ce/>.

364 Method

365 The experiment included two separate tasks: The principal picture-word task was
366 preceded by a localiser task to account for between-participant variability in the N1's
367 timing and location. The details of stimulus selection and control as well as presentation

368 timing are provided in the following sections. For clarity, we first introduce the overall
369 Congruency-Predictability design of the picture-word task. In this task, pictures of single
370 objects are presented, followed by a noun, and participants decide whether the noun
371 corresponds to the object. The level of Predictability of the noun was determined from
372 norms of possible terms used to label a set of individual pictures (Brodeur et al., 2014).
373 The most frequent, modal name agreement varied across pictures. Thus, level of noun
374 Predictability was continuous and varied between 7% and 100%. The Congruency of the
375 noun was either congruent (matching the modal name of the picture) or incongruent (a
376 semantically unrelated noun matched across several lexical variables).

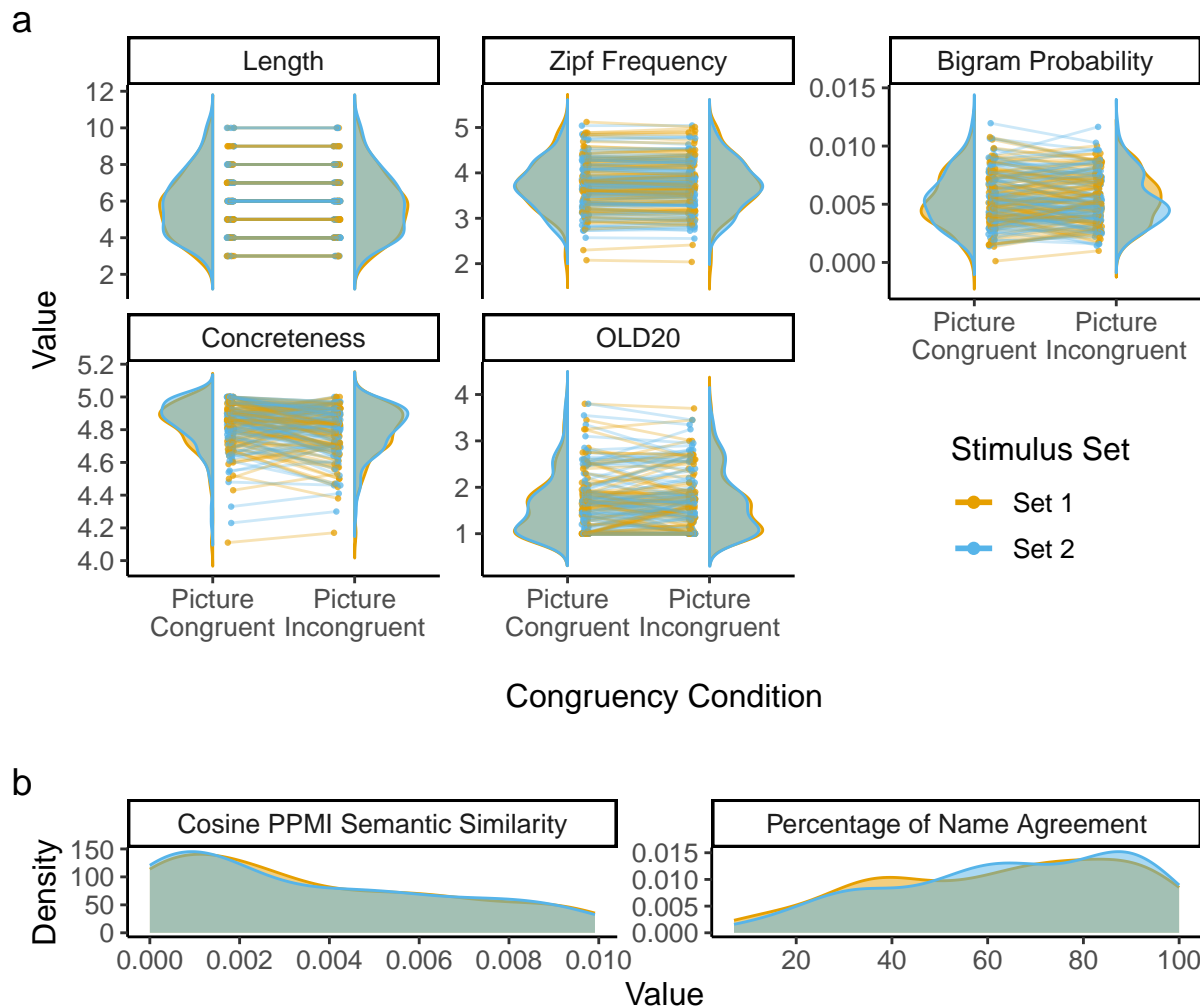
377 **Materials: Picture-Word Task**

378 A total of 400 words were selected with LexOPS (Taylor et al., 2020), a package for
379 the generation and control of lexical variables in the R programming language (R Core
380 Team, 2021). There were 200 words per Congruency condition, with one congruent and one
381 incongruent word per image. A list of the full set of stimuli is available in **Supplementary**
382 **Materials A**. The experimental stimuli are summarised in **Figure 4**. First, stimuli were
383 filtered according to norms collected by Brysbaert et al. (2019), such that at least 90% of
384 participants knew each word. In addition, stimuli were filtered such that all words were
385 nouns according to the dominant part of speech data from SUBTLEX-UK (van Heuven
386 et al., 2014), and had a mean concreteness rating above 4 (on a Likert scale from 1, least
387 concrete, to 5, most concrete) according to Brysbaert et al. (2014). Images were taken from
388 the Bank of Online Standardised Stimuli (BOSS) norms (Brodeur et al., 2014), a large
389 database of images with normed statistics, including percentage of name agreement, which,
390 critically, we used as a measure of Predictability. Words were identified as possible
391 picture-congruent words if they were listed as the most frequent (i.e., modal) name for any
392 image in the BOSS norms, and were identified as possible picture-incongruent words if they
393 were not.

394 Picture-congruent and -incongruent words were matched item-wise across five

Figure 4

Summary of the picture-word stimuli.



Each panel depicts how a single variable was controlled. (a) Probability densities for variables which were matched item-wise between picture-congruent and picture-incongruent conditions, and distribution-wise between counterbalanced stimulus Sets 1 (in *yellow*) and 2 (in *blue*). Points representing pairs of words which are matched item-wise are joined by lines. Points' positions are jittered slightly along the x-axis for visibility. (b) Probability densities for two variables matched only in a distribution-wise manner between the counterbalanced stimulus sets: Cosine PPMI (Positive Pointwise Mutual Information) Semantic Similarity from SWOW (Small World of Words; De Deyne et al., 2019), and modal name agreement from the BOSS norms. These variables cannot be matched between Congruency conditions because only a single value describes each matched congruent-incongruent word pair.

395 lexical variables, with specific tolerance ranges, as follows: (1) word length (number of
396 characters), exactly; (2) concreteness according to Brysbaert et al. (2014), within ± 0.25 ; (3)

397 Zipf frequency (a logarithmic scale of word frequency) according to SUBTLEX-UK, within
398 $\pm.125$; (4) character bigram probability (calculated from SUBTLEX-UK), within $\pm.0025$;
399 and (5) OLD20 (the average Orthographic Levenshtein Distance of the 20 closest
400 neighbours to a given word; Yarkoni et al., 2008) calculated from the LexOPS inbuilt
401 dataset, within $\pm.75$. To ensure that picture-incongruent words were not inadvertent
402 possible descriptors for images, the cosine positive pointwise mutual information (PPMI)
403 measure of associative semantic similarity calculated from the Small World of Words
404 (SWOW) word association norms (De Deyne et al., 2019) was minimised to be $\leq.01$
405 between each image's matched picture-congruent and picture-incongruent words. To ensure
406 picture-incongruent words did not share orthographic features with their respective
407 picture-congruent words, orthographic Levenshtein distance between matched items was
408 maximised. As items were also matched in word length, this meant all matched pairs of
409 words had a Levenshtein distance equal to their number of characters. The variable used to
410 index the Predictability of picture-congruent words was percentage of modal name
411 agreement, which was sampled pseudo-randomly (picture-congruent words were not
412 selected if no incongruent match could be identified fitting the constraints specified above)
413 from the BOSS norms, and varied continuously in the generated stimuli from 7 to 100%.

414 As the participants were recruited in the United Kingdom, possible congruent and
415 incongruent picture-word pairs were excluded if we identified the words as less frequent in
416 British English (e.g., *sidewalk*) or if they were modal names for images that the Canadian
417 participants of the BOSS norms are likely to have been more able to name or distinguish
418 (e.g., *buffalo*, *bison*). In addition, picture-word pairs were excluded if words were identified
419 as shortened versions of nouns (e.g., *limo*, *chimp*) or alternate names for the same object
420 (e.g., *motorbike*, *motorcycle*). Candidate picture-incongruent words were additionally
421 excluded if images were not representative of the images in the BOSS (e.g., *waiter* or
422 *church*, as there were no other images of people or entire buildings in the BOSS), or if they
423 were unimageable despite their high concreteness value (e.g., *item*). Plural words (e.g.,

424 *sticks*) were excluded, as most images in the BOSS have modal names that are singular.
425 Finally, four images with modal names *nut*, *trumpet*, *spinach*, and *tuba* were excluded, as
426 we judged these names to be incorrect descriptions of their images.

427 To avoid repetition effects, each image was presented once, with participants
428 viewing either the associated picture-congruent or picture-incongruent word. This was
429 counterbalanced by splitting the stimuli pseudo-randomly into two equally sized stimulus
430 sets, referred to as Set 1 and Set 2. Each participant was presented with only one of these
431 stimulus sets. Pictures followed by congruent words in Set 1 were followed by incongruent
432 words in Set 2, and vice versa. To minimise any systematic difference between the
433 counterbalanced groups, the split of stimuli was selected to maximise the empirical
434 distributional overlap (Pastore & Calcagni, 2019) between the two stimulus sets in relevant
435 variables. Specifically, the stimulus sets were selected from 50,000 random splits to
436 maximise the overlap between the distributions of the following seven variables: (1)
437 percentage of modal name agreement according to the BOSS norms; (2) cosine PPMI
438 semantic similarity according to the SWOW; (3, 4) Zipf word frequency and character
439 bigram probability according to SUBTLEX-UK; (5) word concreteness (Brysbaert et al.,
440 2014); (6) word length; and (7) OLD20. Variables that were also matched item-wise
441 between the conditions were matched distribution-wise separately within each Congruency
442 condition. This ensured there were minimal systematic differences in distributions between
443 conditions or stimulus sets.

444 To generate stimuli for practice trials, 20 matched pairs of picture-congruent and
445 -incongruent words were generated using the same pipeline as above, except that word
446 frequency, word concreteness, and character bigram probability were not matched
447 item-wise. The practice stimuli were generated from images and words not used in the
448 experimental stimuli. The same practice trials were presented to all participants.

449 Before embarking on the electrophysiological picture-word experiment, we first ran a
450 proof-of-concept behavioural experiment using a different stimulus set generated from a

451 very similar pipeline. We anticipated that increased Predictability should cause faster
452 response time (RT) for congruent trials and have either no effect or a minimal effect on
453 performance for incongruent trials. The results from this behavioural validation are
454 presented in **Supplementary Materials B**. In short, we observed the pattern of results
455 consistent with our expectations, with Predictability leading to faster RTs for congruent
456 trials, but having almost no effect on incongruent trials.

457 **Materials: Localiser Task**

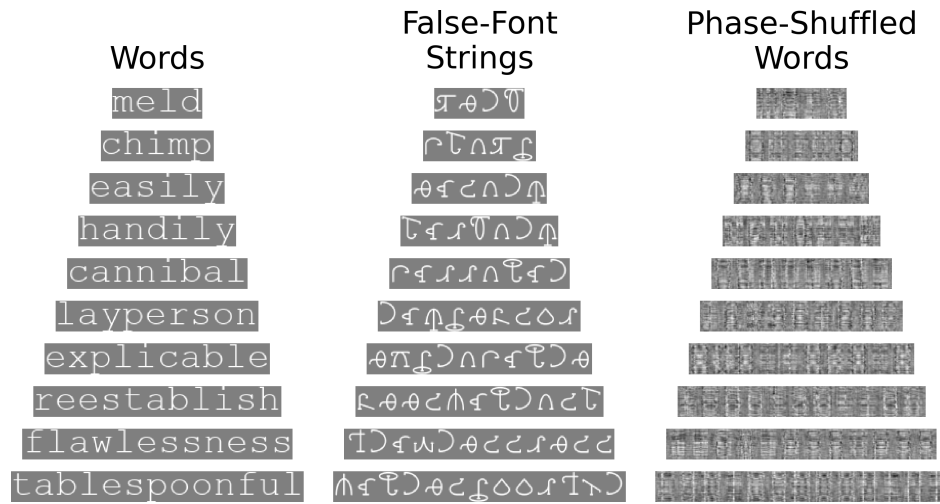
458 The precise location of the N1, and timing of its peak amplitude, is known to vary
459 across studies and among participants. As such, we did not specify a common N1 electrode
460 or timepoint shared among all participants before data collection. Instead, we employed a
461 localiser task to identify, within an appropriate region and time period of interest, the
462 electrode and timepoint at which each participant's maximal sensitivity to orthography
463 emerges (i.e., more extreme amplitudes for words than false-font stimuli). This data could
464 then be used to extract N1 amplitudes in the picture-word task, while accounting for
465 variability among participants in timing and topography of orthographic processes.

466 For the localiser task, three categories of stimuli were presented for 100 trials each
467 (**Figure 5**). These consisted of matched triplets of words (Courier New font), false-font
468 strings (BACS2serif font), and phase-shuffled words. The comparison between words and
469 false-font strings is a standard measure of N1 sensitivity to orthography, with previous
470 evidence suggesting a more robust difference than exists between nonwords and words
471 (Brem et al., 2018; Maurer, Brandeis, et al., 2005; Pleisch et al., 2019). However,
472 phase-shuffled words were employed as an alternative comparison for exploratory analyses,
473 with equal spatial-frequency amplitude and permuted spatial-frequency phase. Similar
474 phase-shuffled word stimuli have shown robust differences to word forms in fMRI
475 investigations of vOT activity (Rauschecker et al., 2012; Rodrigues et al., 2019; White
476 et al., 2019; Yeatman et al., 2013).

477 To generate the localiser stimuli, a large list of suitable words ($N=27,332$) was

Figure 5

Ten example stimuli for each stimulus type in the localiser task.



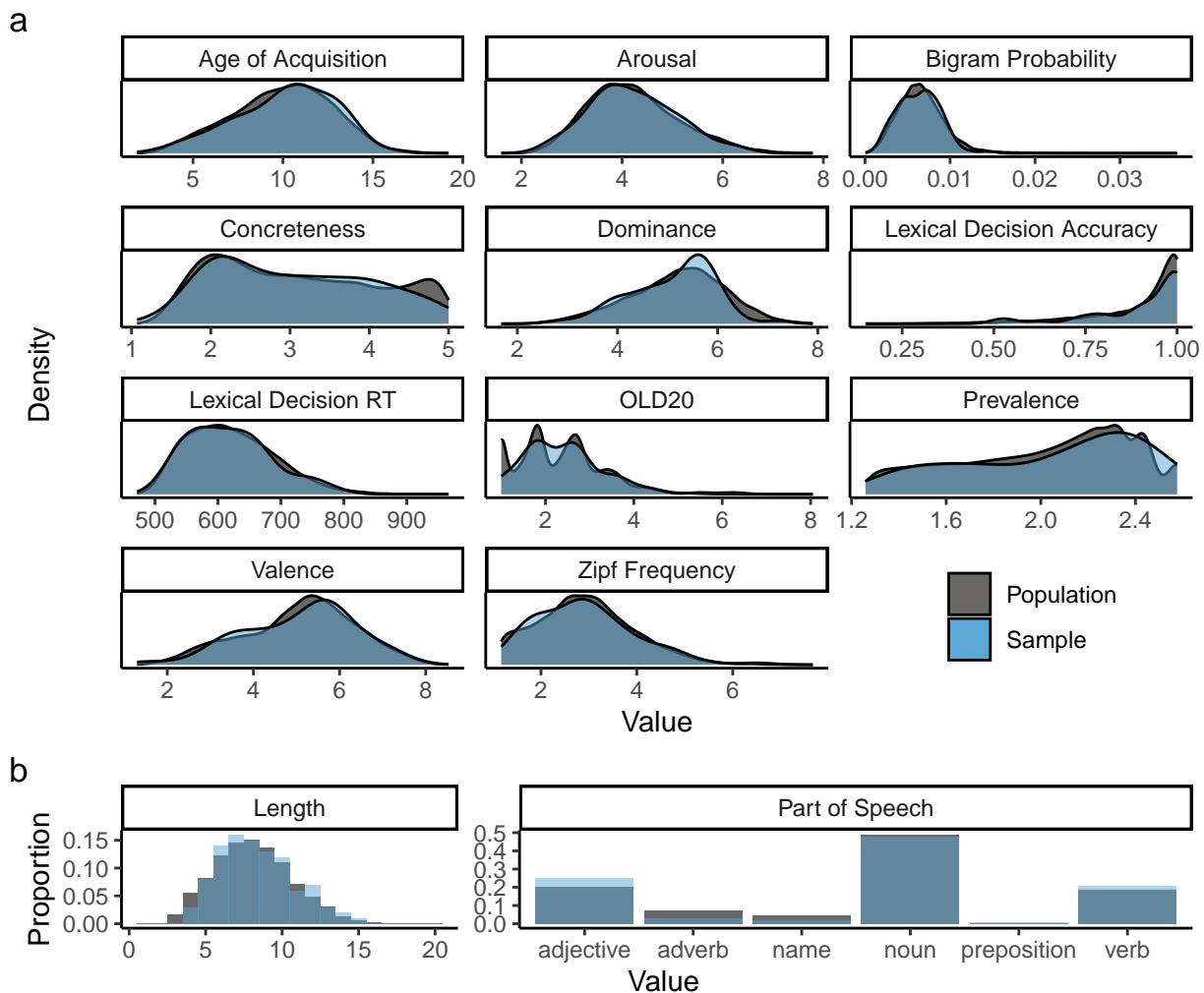
Each row represents a matched triplet of word, false-font string, and phase-shuffled word stimuli. The phase-shuffled word images were generated uniquely for each trial.

478 identified by filtering the word prevalence norms of Brysbaert et al. (2019) to only contain
479 words known by at least 90% of participants and which were not selected for the main
480 experiment. A representative sample ($N=100$) of this list was generated by maximising
481 distributional overlap (Pastore & Calcagni, 2019), between the sample and the full list of
482 candidates, on 13 variables where observations were available: (1) word prevalence
483 (Brysbaert et al., 2019); (2) length (number of characters); (3) word frequency in Zipf in
484 SUBTLEX-UK (van Heuven et al., 2014); (4) part of speech according to SUBTLEX-UK;
485 (5) character bigram probability calculated from SUBTLEX-UK; (6) OLD20 (Yarkoni
486 et al., 2008) calculated from the LexOPS dataset (Taylor et al., 2020); (7) concreteness
487 (Brysbaert et al., 2014); (8) age of acquisition (Kuperman et al., 2012); (9, 10) average
488 lexical decision response time (RT) and accuracy according to the British Lexicon Project
489 (Keuleers et al., 2012); and (11, 12, 13) the emotion ratings of valence, arousal, and
490 dominance (Warriner et al., 2013). Similarity in the categorical variable of part of speech
491 was maximised with dummy-coded variables (0 or 1 for absence or presence of a category,
492 respectively). Distributional similarity across all variables was maximised by selecting from
493 500,000 random samples the sample with the highest total distributional overlap with the

494 full list of possible words. Distributions of the selected sample of words are summarised in
495 **Figure 6**. The full list of stimuli for the localiser task is presented in **Supplementary**
496 **Materials C**.

Figure 6

Distributions of key variables illustrate the similarity between the selected localiser stimuli words (sample) and the list of words from which they were drawn (population).



Panel **a** shows distributional similarity of continuous variables. Panel **b** shows similarity in length (all integer values) as a histogram showing proportions, and the similarity in the counts of each part of speech category as a bar plot of proportions. Only the part of speech categories which were present in the sample are shown. No members of less common part of speech categories, such as determiner or number, were selected in the sample.

498 Set (BACS; Vidal et al., 2017) in BACS2serif font. In this way, we had an item-wise
499 false-font match to each word, where every Courier New character in the word stimuli is
500 replaced with a BACS character matched in the number of strokes, junctions, terminations,
501 and serifs. The phase-shuffled stimuli were generated by using a Fourier transformation to
502 extract the phase and amplitude from the word images. Phase values were randomly
503 shuffled (i.e., permuted), such that the overall distribution of phase could be preserved,
504 while amplitude values were unchanged. An inverse Fourier transformation was then used
505 to generate a new image with the original amplitude values, but with phase randomly
506 shuffled. To prevent phase shuffling from producing noticeably large changes in contrast,
507 the phase shuffling was done on a version of the word image with 50% of the original
508 contrast. After the inverse Fourier transformation, the contrast of the generated
509 phase-shuffled image was readjusted to equal that of the original word image. To avoid
510 repeating the same stimuli across participants more than necessary, unique phase-shuffled
511 images were generated for each trial, for each participant.

512 Versions of the localiser task's stimuli were also created in green, to signal the
513 participant to respond. For words and nonwords, this was done by simply changing the
514 font colour to green. To preserve image intensity, the colour of phase-shuffled images was
515 changed by altering pixels in the following way. For pixels in which the value in the green
516 channel was less than 50% of the maximum intensity (i.e., the intensity of all channels in
517 the grey background), values in red and blue channels were altered to equal the value in
518 the green channel for that pixel. For all other pixels, the values in red and blue channels
519 were set to 50% of the maximum intensity.

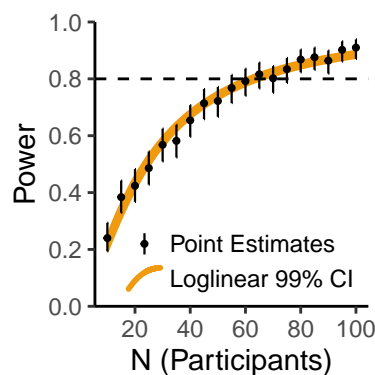
520 **Participants**

521 The sample size of 68 participants was decided via a power analysis using
522 Monte-Carlo simulations of a realistic effect size (**Supplementary Materials D**). This
523 revealed that with ≥ 68 participants we could expect $>80\%$ statistical power in the long
524 run (**Figure 7**). All 68 participants (40 female, 27 male, 1 non-binary) were monolingual

525 native English speakers. Participants were randomly allocated into one of the four
526 combinations of stimulus set (Set 1, Set 2) and response group (i.e., the left-right mapping
527 of the two response buttons for affirmative and negative responses), such that each
528 combination of stimulus set and response group comprised 17 participants. No participants
529 reported diagnosis of any reading disorder. Ages ranged from 18 to 37 years ($M=22.69$,
530 $SD=4.9$), and all participants reported having normal or corrected-to-normal vision.
531 Participants' handedness was assessed via the revised short form of the Edinburgh
532 Handedness Inventory (Veale, 2014), with participants only permitted to take part if they
533 scored a laterality quotient of $+40$ indicating right handedness. Exclusion criteria for
534 participants were determined prior to data collection as follows: (1) if 10 or more channels
535 showed an offset more extreme than ± 25 mV (as measured on the BioSemi acquisition
536 software, ActiView), or (2) if more than 5% of the trials were lost due to technical issues
537 with the EEG system. As no participants satisfied these criteria, no participants were
538 excluded after data collection. Data collection was approved by the Ethics Committee of
539 the institution at which the data were collected (application number: 300200117).

Figure 7

Estimated relationship between number of participants and statistical power.



Black points and error bars depict point estimates $\pm 99\%$ Binomial confidence intervals, each from 500 simulations. As 500 simulations provides a noisy estimate, we interpolated the relationship between N and power via a loglinear, logit-link Binomial model. The *orange* region depicts the 99% confidence intervals of this loglinear model.

540 **Procedure**

541 Stimuli were presented on a VPixx Technologies VIEWPixx screen (resolution
542 1920*1080 pixels, diagonal length 23", model VPX-VPX-2004A). Participants completed
543 the experiment on a chin rest positioned 48 cm from the centre of the screen. Stimuli were
544 presented on a grey background equal to 50% of the maximum intensity in each colour
545 channel, roughly 12.3 cd/m². The experiment was written using the Python library
546 PsychoPy (Peirce, 2007), and all code and materials are available in the repository
547 associated with the study. All stimuli were presented centrally (horizontally and
548 vertically). All trials in both tasks were presented in a pseudo-randomised order, such that
549 no more than five consecutive trials required the same response from the participant. Trials
550 were randomised across blocks, with the exception of the practice block, for which trials
551 were randomised within the one block.

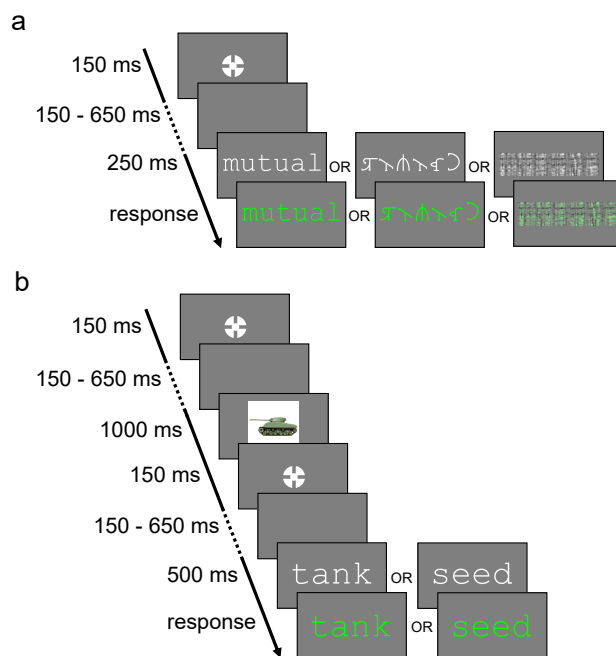
552 A mistake in the lab setup, which we discovered after data collection, meant that
553 the display screen was running at 120 Hz rather than an expected 60 Hz. As we were
554 controlling stimulus presentation by screen refreshes, this meant that all our stimuli were
555 presented for half the expected durations. For this reason, the veridical stimulus durations
556 described here differ from those described in the pre-registration.

557 Participants started with the localiser task, in the form of a lexical decision task
558 (**Figure 8a**). The localiser task began with 30 practice trials, and was then followed by
559 300 trials split into 5 blocks of 60 trials. Each trial began with the bullseye fixation target
560 recommended by Thaler et al. (2013) (outer and inner circle diameters were 0.6° and 0.2°
561 of visual angle), presented for 150 ms. This was followed by a jittered interval of between
562 150 and 650 ms, during which the screen was blank. The stimulus (word, false-font string,
563 or phase-shuffled word image) was then presented at a height of 1.5° (width of 1.07° for one
564 character). Words and false-font strings were presented in white (80 cd/m²), in the
565 respective fonts of non-proportional Courier New and BACS2serif font. The stimulus was
566 visible for 250 ms, after which the font colour changed to green to signal participants to

567 respond. Participants were requested to respond once after the stimulus changed colour,
568 quickly and accurately, to indicate whether the stimulus they saw in each trial was either a
569 word or not a word. The stimulus remained on screen until the participant responded.
570 Responses were given with the right and left control ('Ctrl') keys of a QWERTY keyboard,
571 with the mapping of affirmative and negative responses counterbalanced across
572 participants. After the participant had responded, there was a delay of around 100 ms
573 (variable as data was saved to disk during this interval), and then the next trial began.

Figure 8

Trial structure of the (a) localiser task and (b) picture-word task.



This figure is illustrative and the sizes are not to scale; in the experiment, images were in fact presented at a much larger scale than words.

574 After the localiser task, participants completed the picture-word task (**Figure 8b**),
575 comprising an initial practice block of 20 trials, followed by 200 trials split into 5 blocks of
576 40 trials. As in the localiser task, each trial in the picture-word task began with the
577 bullseye fixation point, presented for 150 ms, after which there was a blank screen for a
578 jittered interval of between 150 and 650 ms. An image was then presented for 1000 ms, at
579 a size of 10x10°. The bullseye fixation point was then presented again for 150 ms, followed

580 by another interval jittered between 150 and 650 ms. The word was then presented in
581 white Courier New font, at a height of 1.5° (width 1.07° for one character). After 500 ms,
582 the word turned green, and participants could provide their response to indicate whether
583 the word described the image they saw. The word remained on screen until the participant
584 responded. As in the localiser task, responses were given with the right and left control
585 ('Ctrl') keys of a QWERTY keyboard, with the mapping of affirmative and negative
586 responses counterbalanced across participants, but kept consistent within participants
587 across the two tasks. After participants had responded, there was a delay of around 100 ms
588 (again, variable as data was saved to disk during this interval), and then the next trial
589 began. There was no deadline for participants to respond. The instructions given to
590 participants for the picture-word task are presented in **Supplementary Materials E**.

591 The first blocks of both tasks consisted of practice trials with 10 exemplars for each
592 stimulus type (word or false-font string or phase-shifted image, and congruent or
593 incongruent noun for the localiser and picture-word tasks, respectively), during which
594 participants were additionally given immediate feedback on their accuracy for each trial.
595 These practice trials were followed by green text reading "CORRECT!" if the participant
596 responded correctly, or else by red text reading "INCORRECT!", presented in Courier New
597 font with a height of 1.5°, for 1000 ms. Participants had self-paced breaks between blocks
598 for each task. Before the practice trials and at the start of every experimental block,
599 participants were presented with instructions for the task (available in **Supplementary**
600 **Materials E**), summarising what would occur in each trial, and specifying that they
601 should respond as quickly and accurately as possible once the stimulus turned green. These
602 instructions also specified which keys participants should press to indicate their decision.
603 After each experimental block, including the practice trials, participants were presented
604 with their average accuracy and median response time. After the practice trials,
605 participants were additionally given the option to run the practice trials again. In the
606 experimental blocks, no trial-level feedback was provided.

607 **Recording**

608 EEG data were recorded using a 64-channel BioSemi system, sampling at 512 Hz,
609 with an online low-pass filter at the Nyquist frequency. Electrodes were positioned in the
610 standard 10-20 system locations. Four electro-oculography (EOG) electrodes were placed
611 to record eye movements and blinks: 2 were placed to the sides of eyes (on the right and
612 left outer canthi), and 2 below the eyes (on the infraorbital foramen). Electrode offset was
613 kept stable and low through the recording, within ± 25 mV, as measured by the BioSemi
614 ActiView EEG acquisition tool. Electrodes whose activity exceeded this threshold were
615 recorded but were removed (and interpolated) in data preprocessing.

616 **Preprocessing**

617 The following section details the procedure applied to EEG data from each
618 individual session, with the same pipeline being applied to both the localisation task and
619 picture-word task unless otherwise specified. EEG preprocessing was achieved using
620 functions from the EEGLAB (Delorme & Makeig, 2004) toolbox for MATLAB (MATLAB,
621 2022) or OCTAVE (Eaton et al., 2020). For both tasks, trials were excluded if responded to
622 incorrectly ($N=368$, or .02%, in localiser task, $N=226$, or .02%, in picture-word). Further
623 trials were excluded if responded to later than 1500 ms after the word (or nonword)
624 changed colour ($N=41$, or .002%, in localiser task, $N=42$, or .003%, in picture-word).

625 Channels recorded as having offsets ± 25 mV during data acquisition were removed
626 from the data (in both tasks, 56 channels, or 1.27%, were removed across all participants),
627 with their activity to be later interpolated. The EEG data were then re-referenced to the
628 average activity across all electrodes and filtered with a 4th order Butterworth filter
629 between .1 and 40 Hz. To counteract the distortion in signals' timing (phase) that is
630 inherent to causal filters, the filter was applied in both directions (i.e., two-pass), with the
631 MATLAB function, *filtfilt()*. In our pre-registration, we specified that we would apply a
632 Butterworth filter with a bandpass of .5-40 Hz. However, after the pre-registration, we
633 considered that, consistent with research into the effects of high-pass filters (Rousselet,

634 2012; Tanner et al., 2015; VanRullen, 2011), this could produce artefactually early effects.
635 As a result, we lowered the high-pass filter to a less problematic .1 Hz. For comparison,
636 demonstrating that our change to the pre-registered pipeline had minimal effect on the
637 results or our conclusions, the results using the original filter are presented in
638 **Supplementary Materials F**.

639 Segments of data outside of experimental blocks (i.e., in break periods) were
640 identified and removed so they did not impact the independent components analysis (ICA)
641 applied later in the pipeline. Blocks were identified as beginning 500 ms before stimulus
642 presentation in the first trial of each block, ending 500 ms after the end of the last trial's
643 epoch. To reduce the impact of occasional non-stationary artefacts with high amplitude
644 (such as infrequent muscle movements), artefact subspace reconstruction (ASR; Chang
645 et al., 2020) was used with a standard deviation cutoff of 20 to remove non-stationary
646 artefacts. Following this, an ICA was run on the data to identify more stationary artefacts.
647 The ICA was run using the FastICA algorithm (Hyvärinen & Oja, 1997), with a recorded
648 random seed for reproducibility. The ICA was run on a copy of the data with channel
649 offsets removed to allow for better sensitivity to electro-oculogram (EOG) artefacts
650 (Groppe et al., 2009). The ICLabel classifier (Pion-Tonachini et al., 2019) was used to
651 automatically identify artefacts which were eye- or muscle-related. Components classified
652 by ICLabel as eye-related or muscle-related with a probability of $\leq 85\%$ were removed from
653 the data. Following eye movement artefact removal, activity from channels which were
654 removed was interpolated via spherical splines (Localiser: $M=1.14$ per participant,
655 $SD=1.58$; Picture-Word: $M=1.68$, $SD=2.03$), as implemented in EEGLAB. Trials were
656 then epoched and baseline-corrected to the 200 ms preceding stimulus presentation. For
657 the localiser task, stimulus presentation refers to the time point at which words, false-font
658 strings, or phase-shuffled images were presented; in the picture-word task, stimulus
659 presentation refers to the target word.

660 For the planned analysis, we pre-registered an approach to maximise sensitivity to

661 effects of Congruency and Predictability on the N1. To encompass the typical topography
662 and timing of the posterior left-lateralised N1, we selected eight occipitotemporal
663 electrodes (**Figure 9**; electrodes O1, PO3, PO7, P5, P7, P9, CP5, and TP7) and a 120-200
664 ms window. In contrast to some previous studies whose N1 windows extended beyond 200
665 ms, we set 200 ms as an upper bound for the possible maximal timepoint in the main
666 analysis, to ensure effects were indeed restricted to the N1, and not later components like
667 the N400. For each participant, we identified the electrode that showed maximal sensitivity
668 to orthographic information in the N1 during the localisation task. Specifically, each
669 participant’s “maximal electrode” (within the region of interest and selected time window)
670 was the one which showed the largest mean amplitude difference, in the expected direction,
671 across all localiser trials between word and false-font string stimuli. The expected direction
672 was a more negative-going N1 for words than for false-font strings, a pattern based on
673 previous findings (Appelbaum et al., 2009; Bentin et al., 1999; Eberhard-Moscicka et al.,
674 2016; Pleisch et al., 2019; Zhao et al., 2014). Each participant’s “maximal timepoint” was
675 the timepoint at which the maximal electrode showed the greatest sensitivity to the
676 word-versus-false-font difference in the expected direction. Each participant’s maximal
677 electrode and maximal timepoint were then used to extract their trial-level N1 amplitudes
678 from the picture-word task. To reduce the influence of noise on trial-level data, the
679 trial-level N1 amplitudes in the picture-word task were calculated as the maximal
680 electrode’s mean amplitude across 3 timepoints: the participant’s maximal timepoint, and
681 the timepoints immediately preceding and following it. At the recorded sample rate of 512
682 Hz, this is equivalent to a window of 5.85 ms (i.e., $1/512 \times 3$) centred on the maximal
683 timepoint.

684

Results

685

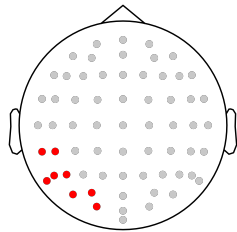
686

687

The planned analysis (pre-registered at <https://osf.io/jk3r4>) examined whether the hypothesised effect of a Predictability-dependent reduction of N1 amplitudes for picture-congruent words was observed at the electrode/timepoint in which each participant

Figure 9

The left-lateralised occipitotemporal region of interest selected for the N1 (highlighted in red).



688 showed maximal sensitivity to orthography. We then present exploratory analyses, which
689 respectively examine the Bayesian probability that our data are consistent with the
690 hypothesis, and delineate the time-course of the Congruency-Predictability interaction. We
691 also conducted exploratory behavioural analyses, which we report in the supplementary
692 materials, examining behavioural results in the picture-word study (**Supplementary**
693 **Materials G**), and EEG and behavioural results from the localiser task (**Supplementary**
694 **Materials H**)

695 **Planned Analysis**

696 The planned analysis tested the pre-registered hypothesis of a
697 Congruency-Predictability interaction in which N1 amplitudes are reduced (i.e., less
698 negative going) for picture-congruent trials than for picture-incongruent trials, and in
699 which this difference is greatest at the highest levels of predictability, and smallest at the
700 lowest levels of predictability. This was based on the notion that the N1 indexes prediction
701 error in biasing contexts. We did not find evidence in favour of this hypothesis.

702 The trial-level N1 amplitudes from the picture-word task were modelled using a
703 linear mixed-effects model fit with the R package *lme4* (Bates et al., 2015), estimating the
704 maximal random effects structure justified by the experiment's design (Barr et al., 2013) as
705 detailed in the section on the power analysis. The model was fit using the *bobyqa* optimiser
706 (Powell, 2009). In *lme4* syntax, the formula for the mixed-effect model was specified as:

707 `amplitude ~ 1 + congruency * predictability +`

708 (1 + congruency * predictability | participant_id) +
709 (1 + congruency | image_id) +
710 (1 | word_id)
711

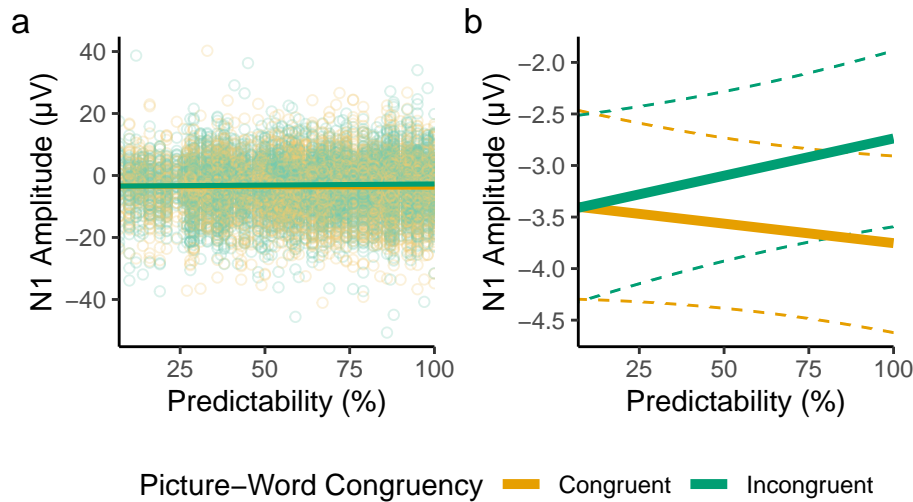
712 In this formula, *amplitude* is the trial-level N1 amplitude in microvolts, while
713 *congruency* is a deviation-coded categorical variable indicating whether a given trial's word
714 was picture-congruent or -incongruent, and *predictability* refers to the proportion of name
715 agreement in the BOSS norms, normalised between 0 and 1. A consequence of this coding
716 method is that the model's intercept reflects the predicted amplitude at the lowest level of
717 Predictability, averaged across both levels of Congruency, while the slopes' coefficients are
718 standardised and directly comparable in their magnitude. The variables of *participant_id*,
719 *image_id*, and *word_id*, in the formula, identify each trial's participant, image, and word,
720 respectively.

721 The fixed effect relationships predicted by the model are presented in **Figure 10**.
722 The model intercept, reflecting the average N1 amplitude at the lowest level of
723 Predictability, was estimated to be $\beta = -3.35 \mu\text{V}$ ($SE = .50$). The fixed effect of Congruency
724 from this model was estimated as $\beta = -.02 \mu\text{V}$ ($SE = .32$), which captures that, at the lowest
725 level of Predictability (7%), N1 components for picture-congruent and -incongruent words
726 were estimated to be very similar (.02 μV difference). The main effect of Predictability was
727 estimated as $\beta = .16 \mu\text{V}$ ($SE = .29$), meaning that N1 amplitudes, averaged across congruent
728 and incongruent conditions, were only .16 μV less negative-going at the highest level
729 (100%) than at the lowest level of Predictability (7%). The effect of interest, the
730 interaction between Congruency and Predictability, was in the opposite direction from that
731 hypothesised, estimated as $\beta = -1.02 \mu\text{V}$ ($SE = .50$). As the polarity of our predictions was
732 explicitly specified, we interpret these results as a failure to find evidence in favour of the
733 hypothesis.

734 To describe the estimated interaction, for picture-incongruent words, the effect of
735 Predictability was estimated to be $\beta = .66 \mu\text{V}$ ($SE = .35$), while for picture-congruent words,

Figure 10

Fixed effect predictions from the planned analysis of the picture-word task.



(a) Model-derived fixed-effect predictions, visualised over results from all trials (individual points). (b) Fixed-effect predictions visualised alone for visibility, with dashed lines depicting the bounds of 95% bootstrapped prediction intervals (estimated from 5,000 samples), where bootstrapped predictions were generated using the *bootMer()* function of *lme4*. For feasibility, bootstrapped predictions were generated from a version of the model that lacked random slopes.

736 the effect of Predictability was estimated to be $\beta = -.37 \mu\text{V}$ ($SE = .38$). As such, the slopes
737 for the effect of Predictability in both Congruency conditions were in directions
738 inconsistent with our predictive coding hypothesis.

739 For comparison, we also analysed the data altering aspects of our planned analysis
740 method: first using the maximal electrodes that would be identified from the comparison
741 between words and phase-shuffled words, and second using averages within the
742 occipitotemporal region of interest (**Supplementary Materials I**). These exploratory
743 analyses revealed very similar patterns of effects, with estimates of the
744 Congruency-Predictability interaction similarly inconsistent with our hypothesis, which we
745 derived from a simple predictive coding account of the N1.

746 **Exploratory Bayesian Analysis**

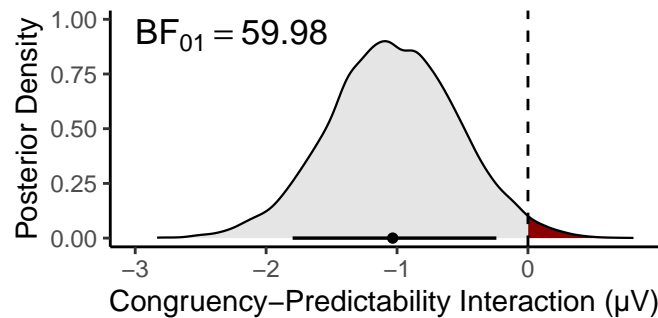
747 We observed a Congruency-Predictability interaction in the opposite direction (i.e.,
748 negative) to what we expected under our predictive coding hypothesis (i.e., positive). To
749 explicitly quantify the probability of our predictive coding hypothesis, we fit a Bayesian
750 implementation of the model described in the planned analysis, in STAN (STAN
751 Development Team, 2023) via *brms* (Bürkner, 2017). This model was fit to the same data,
752 and estimated the same hierarchical formula, with the same Gaussian link function as that
753 described above, but was specified with weakly informative priors for the fixed effects.
754 Specifically, the prior for the fixed effect intercept was specified as a normal distribution of
755 mean -5, and *SD* 10, while all fixed effect slopes' priors were specified as normal
756 distributions centred on 0, with *SDs* of 5. Covariance matrices were assigned flat priors,
757 and default priors for *brms* were used for random effect *SDs* and the sigma parameter of
758 the normal distribution. The model was fit with 5 chains and 5000 iterations per chain
759 (split equally between warmup and sampling) such that there were a total of 12,500
760 posterior samples. Consistent with the linear mixed-effects model we fit via *lme4*, this
761 analysis revealed a median posterior estimate for the Congruency-Predictability interaction
762 of $\beta = -1.03 \mu\text{V}$ (89% highest density interval = [-1.8, -.24]; **Figure 11**). We calculated,
763 given this posterior distribution, that the Congruency-Predictability interaction is 59.98
764 times more likely to be less than 0, than it is to be greater than zero (that is, BF_{01}), which
765 we consider to be strong evidence against our hypothesis.

766 **Exploratory Time-Course Analysis**

767 To examine the time-course of effects, we fit separate linear mixed-effects models to
768 sample level data for the left-lateralised occipitotemporal region of interest, with variables
769 coded as described for the planned analysis. For feasibility, data were downsampled to 256
770 Hz, and the models did not estimate random slopes. To account for variability between
771 electrodes, and for per-participant differences in topography, random intercepts were
772 estimated for each combination of participant and electrode. In *lme4* syntax, the model

Figure 11

Posterior density for the Congruency-Predictability interaction.



The region of the posterior distribution consistent with the predictive coding hypothesis (where $\beta > 0$) is highlighted in red. The point and horizontal line below the density plot depict respectively the median estimate and 89% highest density interval of the posterior distribution.

773 formula was specified as follows:

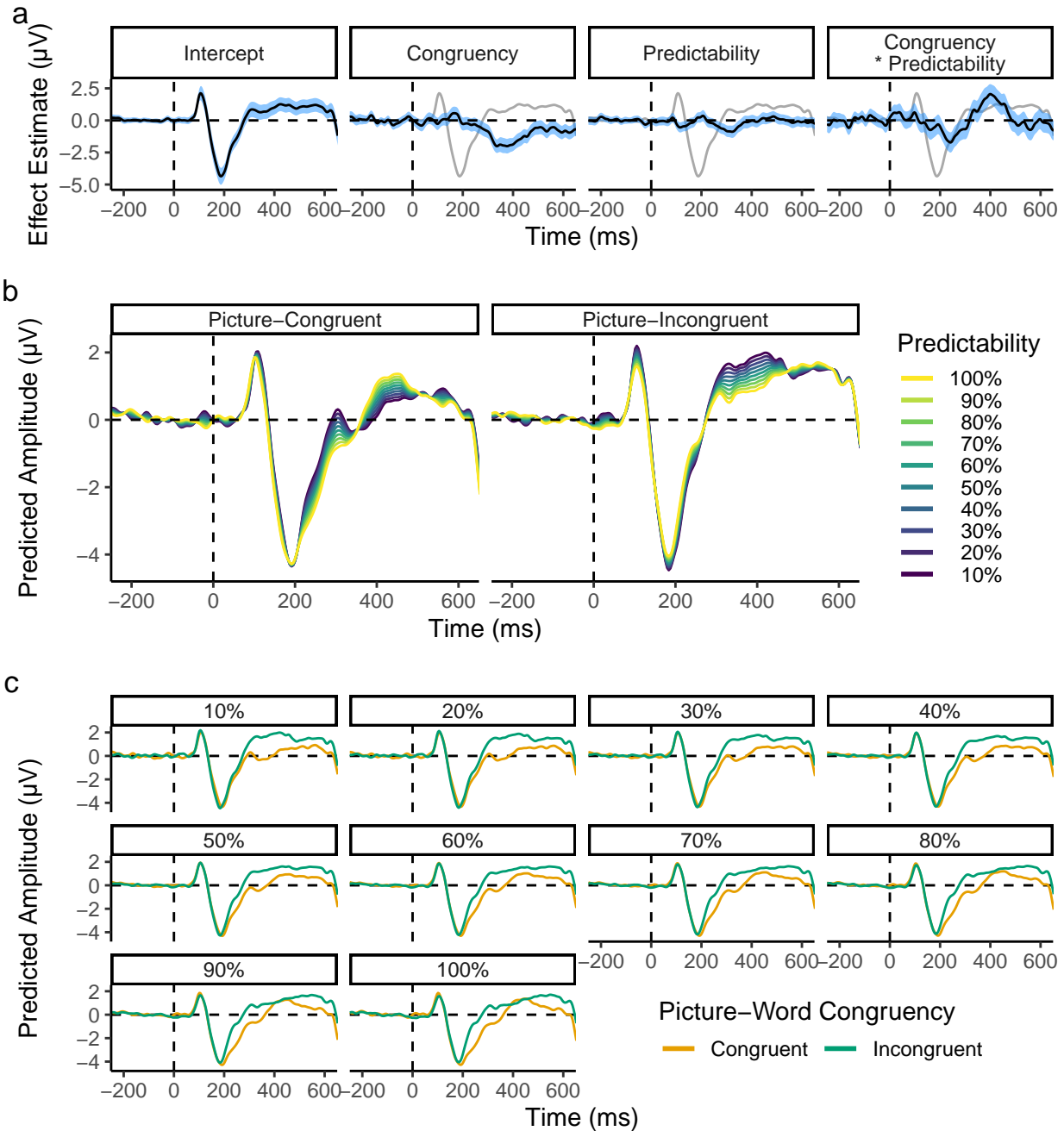
```
774 amplitude ~ 1 + congruency * predictability +  
775     (1 | participant_id) +  
776     (1 | participant_id:electrode_id) +  
777     (1 | image_id) +  
778     (1 | word_id)  
779
```

780 The results (**Figure 12**) reproduced findings from the planned analysis, with
781 increases in Predictability associated with more negative (larger) N1 amplitudes for
782 picture-congruent words, and with less negative (smaller) N1 amplitudes for
783 picture-incongruent words. The Congruency-Predictability interaction of interest remained
784 negative, and thus in the opposite direction to that hypothesised, throughout the N1.

785 The sample-level analysis additionally suggested that the difference was largest in
786 the N1's offset period (succeeding the peak). A later Congruency-Predictability interaction
787 was also observed, peaking at around 400 ms (possibly resulting from effects in the N400
788 component) in the opposite direction to that observed for the N1's offset. To better
789 understand the time-course of the Congruency-Predictability interaction, we examined the
790 time-course of the effect of Predictability for picture-congruent and -incongruent words
791 separately (i.e., simple effects; **Figure 13**). This showed more clearly that Predictability

Figure 12

Time-course of fixed effects from the sample-level analysis of the left-lateralised occipitotemporal region of interest.

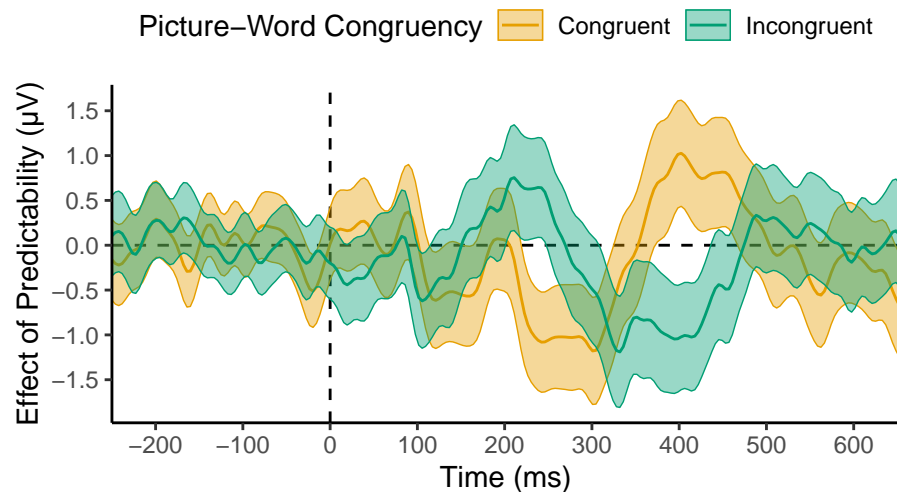


(a) Time-course of fixed effects estimates, with blue-shaded regions depicting 95% confidence intervals. The model intercept (reflecting amplitudes at the lowest level of Predictability) is depicted as a grey line on each panel to provide a reference for timing and magnitude of effects. (b) Fixed-effect predictions for picture-congruent and -incongruent words at levels of Predictability from 10 to 100%, in steps of 10%. (c) Same data as (b), but split by Predictability rather than Congruency.

792 reduced amplitudes in the N1 for picture-incongruent words, but increased amplitudes for
793 picture-congruent words. This difference peaked around 225 ms, but reversed in direction
794 after 300 ms. It is of note that the peak of the observed effects in the N1 was later than
795 originally anticipated (the planned analysis was limited to ≤ 200 ms). Nevertheless, the
796 model intercept (**Figure 12a**) clearly shows that these effects peaked during the N1's
797 offset period.

Figure 13

Time-course of the effect of Predictability for picture-congruent and -incongruent words.



Central lines depict effect estimates, derived from sample-level models that were coded such that the model intercept lay at the respective levels of picture-word Congruency. Estimates reflect ERPs for words at the maximum level of Predictability, minus those at the minimum level of Predictability. Shaded areas depict 95% confidence intervals of model estimates.

Discussion

798
799 In the present study, we tested whether a simple predictive coding account could
800 explain online prediction effects on the amplitude of N1 ERP components elicited by words
801 in biasing contexts. We biased expectations for upcoming words via images of varying
802 predictability. Based on a predictive coding framework, we hypothesised that there would
803 be an interaction between picture-word Predictability and Congruency in which N1
804 amplitude scales with prediction error. Planned analyses failed to find evidence for this
805 hypothesis, and exploratory analyses revealed, despite strong evidence for prediction effects

806 in the N1, that the direction of the interaction was opposite to that expected under the
807 hypothesis. Specifically, increases in Predictability were associated with greater-amplitude
808 N1s for picture-congruent words, and smaller-amplitude N1s for picture-incongruent words.
809 On this basis, we conclude that a simple predictive coding explanation of the N1 cannot
810 explain predictability effects observed in the picture-word verification task used here.

811 In recent years, predictive coding models have been increasingly applied to explain
812 neural phenomena observed during language processing. This includes predictive coding
813 perspectives on the N1 specifically (e.g., Gagl et al., 2020; Huang et al., 2022; Zhao et al.,
814 2019), or its likely generator, vOT (Price & Devlin, 2011), and other areas of language
815 processing. For example, consider the well-researched N400 ERP component, generally
816 recognised since its initial identification as capturing activity related to semantic processes
817 (Kutas & Federmeier, 2011; Kutas & Hillyard, 1980). The N400 shows sensitivity to word-
818 and sentence-level surprise or predictability (Delaney-Busch et al., 2019; Lau et al., 2013;
819 Lindborg et al., 2023; Mantegna et al., 2019; Van Petten & Kutas, 1990), in a manner that
820 may be consistent with predictive coding (Bornkessel-Schlesewsky & Schlewsky, 2019;
821 Eddine et al., 2023; Rabovsky & McRae, 2014). Similar interpretations have been made of
822 other signals, as capturing prediction errors for phonological, semantic, or syntactic
823 representations (Fitz & Chang, 2019; Gagnepain et al., 2012; Van Petten & Luka, 2012;
824 Ylinen et al., 2017; Ylinen et al., 2016). Indeed, emerging evidence supports the broader
825 contention that naturalistic language comprehension utilises a predictive coding hierarchy
826 spanning the language network (Caucheteux et al., 2023; Schuster et al., 2021; Shain et al.,
827 2020).

828 We do not believe our findings refute the existence of predictive coding mechanisms
829 during the N1. Instead, we argue that a simple predictive coding account of the N1, in
830 which the component's amplitude straightforwardly indexes prediction error in a manner
831 dependent on prediction certainty, is insufficient to explain the pattern of effects we
832 observed in the picture-word verification task we used here. For a predictive coding model

833 to better account for these data, it would require elaboration. One feature that may be
834 relevant is the nature of the task. We elected to use a picture-word verification task as it
835 encourages explicit prediction of word forms from non-linguistic contexts. However, this
836 task paradigm may alter predictive processing of word forms in two key ways. First,
837 participants will have soon learned that the observed word form only matches its preceding
838 image 50% of the time, which could have interacted with the effect of Predictability
839 (prediction certainty) in unexpected ways. Second, the requirement for explicit verification
840 of prediction congruency may have encouraged artificial processing strategies that are not
841 representative of naturalistic word recognition and reading processes. To better understand
842 whether and how such factors influence any possible predictive coding effects on the N1, we
843 could manipulate prediction error magnitude and precision while the participant's task
844 instructions do not explicitly require processing of the cue. For instance, we could use a
845 picture-word priming design (Sperber et al., 1979; Vanderwart, 1984), presenting
846 picture-word pairs, as in the current study, but ask participants to respond with lexical
847 decisions. Here, prediction error magnitude could be operationalised as the orthographic
848 distance between the string (whether word or non-word), and precision as the
849 predictability of a word given its picture. We believe that such an approach could provide
850 insight into whether, and which, features of the paradigm we used could have resulted in
851 the unexpected pattern of results. Finally, it is possible that dynamics of predictive
852 processing were influenced by the slow presentation rate employed in the present study,
853 relative to more naturalistic reading paradigms. Indeed, previous research has highlighted
854 the importance of presentation rate in prediction effects during reading (e.g., Dambacher
855 et al., 2012), and recent findings have shown that unpredictability in stimulus presentation
856 timing (e.g., with jittered inter-stimulus intervals) may interfere with predictive processes,
857 as indexed by the mismatch negativity component (Tsogli et al., 2022). This explanation of
858 our results could be tested by study designs examining how the congruency-predictability
859 interaction varies over stimulus onset asynchronies of different durations. In sum, while

860 predictive coding mechanisms may ultimately underlie the pattern of effects we observed,
861 the simple account we have tested requires elaboration, informed by insights from other
862 paradigms, for it to explain why our current pattern of effects is opposite to that expected.

863 Nevertheless, we acknowledge the possibility that the insufficiency of predictive
864 coding accounts to explain the data we observed may reflect a more fundamental
865 shortcoming. To speculate, predictive coding models may account for activity in the N1 in
866 previously tested paradigms without accurately describing the underlying neural processes.
867 For instance, Luthra et al. (2021) showed that, in spoken word recognition, interactive
868 activation models may provide an alternative account of the ERP amplitude reduction
869 observed in response to prediction violations, without invoking key features of predictive
870 coding models. Indeed, effects indicative of predictive processing may emerge in a system
871 that lacks any representations of, or mechanisms implementing, predictions or
872 prediction errors, instead only implementing pattern completion (Falandays et al., 2021).
873 It is tentatively possible that the picture-word verification paradigm we applied here may
874 be a scenario that employs the same neurocognitive processes in the N1 as those employed
875 in other paradigms, but elicits cognitive dynamics whose corresponding neural activity
876 reveals differences from a predictive coding model. It is possible that processing indexed by
877 the N1 can only be explained by a model distinct from the predictive coding framework,
878 even though predictive coding models may correlate with patterns of activity seen in most
879 paradigms. Justifying the development of such a model, distinct from predictive coding,
880 would require much more evidence for the shortcomings of a predictive coding account, and
881 we do not believe our study provides the insights necessary to speculate on the form such a
882 model could take.

883 If a predictive coding account is to explain prediction-driven modulation of activity
884 in the N1, or any component, we believe it is vital for researchers to consider the
885 informational content of representations whose processing is indexed by the component
886 which is thought to capture prediction error. In a hierarchical model of predictive coding,

887 where levels of the hierarchy utilise different representational formats, the interaction
888 between ascending input and descending predictions must involve some mapping of
889 higher-level onto lower-level representations. For instance, if semantic context can influence
890 processing that is closer to sensory input and indexed by early ERP components (e.g.,
891 Enge et al., 2023; Getz & Toscano, 2019; Segalowitz & Zheng, 2009), then higher-level
892 semantic information must be translated into predictions of upcoming lower-level sensory
893 signals. In the case of our study's modulation of the N1, where the N1 is largely implicated
894 in visual-orthographic processing (Bentin et al., 1999; Brem et al., 2018; Ling et al., 2019;
895 Maurer, Brandeis, et al., 2005), predictions of upcoming words must be translated into a
896 visual-orthographic code. Such a mapping could be expected to be very computationally
897 lossy; predictions for visual-orthographic features of a single word should be expected to
898 also confer facilitation for words that are orthographically similar, yet picture-incongruent.

899 From one perspective, mapping of predictions to lower-level representations may be
900 considered a requisite for a phenomenon to be considered top-down modulation (Rauss
901 et al., 2011). This relates to a long-standing debate on whether prediction effects at the
902 lexical level of language processing necessitate top-down input informed by higher-level
903 semantic processes, or could instead result from perhaps more parsimonious intralexical
904 effects (Fodor, 1983; Forster, 1979). A similar argument could be made that context effects
905 on the N1 could be interpreted as intra-*orthographic*, resulting from local interactions in a
906 possible *orthographic module*. As an example, the orthographic features of the word form
907 *fish* may preactivate features of the word form *chips* simply through learned co-occurrence
908 rather than top-down modulation, entirely within an orthographic processing module that
909 possesses nothing approaching a semantic representation. Such facilitation could be
910 implemented via an extension to classic interactive activation models (e.g., McClelland &
911 Rumelhart, 1981) in which there are excitatory lateral connections between word-level
912 units whose strength is determined by co-occurrence frequency. We consider this point to
913 highlight an advantage of paradigms such as ours, that use non-linguistic contexts (e.g.,

914 task instructions, images, etc.) to cue upcoming words and word forms. Effects of context
915 that map across representations in this way necessitate transfer of information across levels
916 of the processing hierarchy, and may thus be considered stronger evidence for an influence
917 of top-down predictions.

918 An aspect of the predictive coding account that our design did not fully test also
919 relates to this idea of representational mapping. We dichotomised the variable of
920 congruency (prediction error magnitude), with orthographic Levenshtein distance
921 maximised between picture-congruent and -incongruent word forms. However, prediction
922 error magnitude should also be expected to vary continuously, from unpredicted word
923 forms that are less to more orthographically similar to the predicted word form. This is
924 comparable to Gagl et al.'s (2020) use of a pixel distance metric to calculate the continuous
925 distance between a presented word form and a context-neutral prior. Such an approach
926 could be applied to biasing contexts by instead calculating the orthographic distance
927 between a presented word form and a context-informed prior, where the probability of
928 observing certain pixels (or orthographic features) could be up-weighted proportional to
929 prediction certainty. We believe such an approach could provide useful insights in
930 elucidating the pattern of effects we observed.

931 In sum, we tested a simple predictive coding account of the word-elicited N1, but
932 failed to find evidence in favour of it. Exploratory analyses suggest that the pattern of
933 effects in the Congruency-Predictability interaction were in the opposite direction to that
934 expected under a simple predictive coding model. We argue that such a model is
935 insufficient to explain the pattern of effects we observed, and we have identified avenues of
936 future research that could better delineate how predictive processes interact with
937 processing during the N1.

References

938

939 Allison, T., McCarthy, G., Nobre, A., Puce, A., & Belger, A. (1994). Human extrastriate
940 visual cortex and the perception of faces, words, numbers, and colors. *Cerebral*
941 *Cortex*, 4(5), 544–554. <https://doi.org/10.1093/cercor/4.5.544>

942 Appelbaum, L. G., Liotti, M., Perez, R., Fox, S. P., & Woldorff, M. G. (2009). The
943 temporal dynamics of implicit processing of non-letter, letter, and word-forms in the
944 human visual cortex. *Frontiers in Human Neuroscience*, 3, 1–11.
945 <https://doi.org/10.3389/neuro.09.056.2009>

946 Barr, D. J., Levy, J., Scheepers, C., & Tily, H. J. (2013). Random effects structure for
947 confirmatory hypothesis testing: Keep it maximal. *Journal of Memory and*
948 *Language*, 68(Supplement), 1–63.
949 <https://doi.org/10.1016/j.jml.2012.11.001.Random>

950 Bates, D., Mächler, M., Bolker, B., & Walker, S. (2015). Fitting linear mixed-effects models
951 using lme4. *Journal of Statistical Software*, 67(1), 1–48.
952 <https://doi.org/10.18637/jss.v067.i01>

953 Bentin, S., Mouchetant-Rostaing, Y., Giard, M. H., Echallier, J. F., & Pernier, J. (1999).
954 ERP manifestations of processing printed words at different psycholinguistic levels:
955 Time course and scalp distribution. *Journal of Cognitive Neuroscience*, 11(3),
956 235–260. <https://doi.org/10.1162/089892999563373>

957 Bornkessel-Schlesewsky, I., & Schlesewsky, M. (2019). Toward a neurobiologically plausible
958 model of language-related, negative event-related potentials. *Frontiers in*
959 *Psychology*, 10(Article 298). <https://doi.org/10.3389/fpsyg.2019.00298>

960 Brem, S., Halder, P., Bucher, K., Summers, P., Martin, E., & Brandeis, D. (2009). Tuning
961 of the visual word processing system: Distinct developmental ERP and fMRI effects.
962 *Human Brain Mapping*, 30(6), 1833–1844. <https://doi.org/10.1002/hbm.20751>

963 Brem, S., Hunkeler, E., Mächler, M., Kronschnabel, J., Karipidis, I. I., Pleisch, G., &
964 Brandeis, D. (2018). Increasing expertise to a novel script modulates the visual N1

- 965 ERP in healthy adults. *International Journal of Behavioral Development*, *42*(3),
966 333–341. <https://doi.org/10.1177/0165025417727871>
- 967 Brodeur, M. B., Guérard, K., & Bouras, M. (2014). Bank of Standardized Stimuli (BOSS)
968 phase ii: 930 new normative photos. *PLoS ONE*, *9*(9), 1–10.
969 <https://doi.org/10.1371/journal.pone.0106953>
- 970 Brysbaert, M., Mandera, P., McCormick, S. F., & Keuleers, E. (2019). Word prevalence
971 norms for 62,000 English lemmas. *Behavior Research Methods*, *51*(2), 467–479.
972 <https://doi.org/10.3758/s13428-018-1077-9>
- 973 Brysbaert, M., Warriner, A. B., & Kuperman, V. (2014). Concreteness ratings for 40
974 thousand generally known English word lemmas. *Behavior Research Methods*, *46*(3),
975 904–911. <https://doi.org/10.3758/s13428-013-0403-5>
- 976 Bürkner, P.-C. (2017). Brms: An R package for Bayesian multilevel models using Stan.
977 *Journal of Statistical Software*, *80*(1), 1–28. <https://doi.org/10.18637/jss.v080.i01>
- 978 Caucheteux, C., Gramfort, A., & King, J.-R. (2023). Evidence of a predictive coding
979 hierarchy in the human brain listening to speech. *Nature Human Behaviour*, 1–12.
980 <https://doi.org/10.1038/s41562-022-01516-2>
- 981 Chang, C. Y., Hsu, S. H., Pion-Tonachini, L., & Jung, T. P. (2020). Evaluation of Artifact
982 Subspace Reconstruction for automatic artifact components removal in
983 multi-channel EEG recordings. *IEEE Transactions on Biomedical Engineering*,
984 *67*(4), 1114–1121. <https://doi.org/10.1109/TBME.2019.2930186>
- 985 Chen, Y., Davis, M. H., Pulvermüller, F., & Hauk, O. (2013). Task modulation of brain
986 responses in visual word recognition as studied using EEG/MEG and fMRI.
987 *Frontiers in Human Neuroscience*, *7*, 1–14.
988 <https://doi.org/10.3389/fnhum.2013.00376>
- 989 Chen, Y., Davis, M. H., Pulvermüller, F., & Hauk, O. (2015). Early visual word processing
990 is flexible: Evidence from spatiotemporal brain dynamics. *Journal of Cognitive
991 Neuroscience*, *27*(9), 1738–1751. https://doi.org/10.1162/jocn_a_00815

- 992 Clark, A. (2013). Whatever next? Predictive brains, situated agents, and the future of
993 cognitive science. *Behavioral and Brain Sciences*, *36*(3), 181–204.
994 <https://doi.org/10.1017/S0140525X12000477>
- 995 Cohen, L., Dehaene, S., Naccache, L., Lehéricy, S., Dehaene-Lambertz, G., Hénaff, M.-A.,
996 & Michel, F. (2000). The visual word form area: Spatial and temporal
997 characterization of an initial stage of reading in normal subjects and posterior
998 split-brain patients. *Brain*, *123*, 291–307.
- 999 Compton, P. E., Grossenbacher, P., Posner, M. I., & Tucker, D. M. (1991). A
1000 cognitive-anatomical approach to attention in lexical access. *Journal of Cognitive*
1001 *Neuroscience*, *3*(4), 304–312. <https://doi.org/10.1162/jocn.1991.3.4.304>
- 1002 Dale, A. M., Liu, A. K., Fischl, B. R., Buckner, R. L., Belliveau, J. W., Lewine, J. D., &
1003 Halgren, E. (2000). Dynamic statistical parametric mapping: Combining fMRI and
1004 MEG for high-resolution imaging of cortical activity. *Neuron*, *26*(1), 55–67.
1005 [https://doi.org/10.1016/S0896-6273\(00\)81138-1](https://doi.org/10.1016/S0896-6273(00)81138-1)
- 1006 Dambacher, M., Dimigen, O., Braun, M., Wille, K., Jacobs, A. M., & Kliegl, R. (2012).
1007 Stimulus onset asynchrony and the timeline of word recognition: Event-related
1008 potentials during sentence reading. *Neuropsychologia*, *50*(8), 1852–1870.
1009 <https://doi.org/10.1016/j.neuropsychologia.2012.04.011>
- 1010 De Deyne, S., Navarro, D. J., Perfors, A., Brysbaert, M., & Storms, G. (2019). Measuring
1011 the associative structure of English: The "Small World of Words" norms for word
1012 association. *Behavior Research Methods*, *51*(3), 987–1006.
1013 <https://doi.org/10.3758/s13428-018-1115-7>
- 1014 Delaney-Busch, N., Morgan, E., Lau, E., & Kuperberg, G. R. (2019). Neural evidence for
1015 Bayesian trial-by-trial adaptation on the N400 during semantic priming. *Cognition*,
1016 *187*, 10–20. <https://doi.org/10.1016/j.cognition.2019.01.001>

- 1017 Delorme, A., & Makeig, S. (2004). EEGLAB: An open source toolbox for analysis of
1018 single-trial EEG dynamics including independent component analysis. *Journal of*
1019 *Neuroscience Methods*, *134*, 9–21. <https://doi.org/10.1016/j.jneumeth.2003.10.009>
- 1020 Dikker, S., & Pylkkanen, L. (2011). Before the N400: Effects of lexical-semantic violations
1021 in visual cortex. *Brain and Language*, *118*(1-2), 23–28.
1022 <https://doi.org/10.1016/j.bandl.2011.02.006>
- 1023 Eaton, J. W., Bateman, D., Hauberg, S., & Wehbring, R. (2020). *GNU Octave version*
1024 *6.1.0 manual: A high-level interactive language for numerical computations*.
1025 <https://www.gnu.org/software/octave/doc/v6.1.0/>
- 1026 Eberhard-Moscicka, A. K., Jost, L. B., Fehlbaum, L. V., Pfenninger, S. E., & Maurer, U.
1027 (2016). Temporal dynamics of early visual word processing - Early versus late N1
1028 sensitivity in children and adults. *Neuropsychologia*, *91*, 509–518.
1029 <https://doi.org/10.1016/j.neuropsychologia.2016.09.014>
- 1030 Eddine, S. N., Brothers, T., Wang, L., Spratling, M., & Kuperberg, G. R. (2023). A
1031 predictive coding model of the N400. <https://doi.org/10.1101/2023.04.10.536279>
- 1032 Enge, A., Süß, F., & Rahman, R. A. (2023). Instant effects of semantic information on
1033 visual perception. *Journal of Neuroscience*.
1034 <https://doi.org/10.1523/JNEUROSCI.2038-22.2023>
- 1035 Falandays, J. B., Nguyen, B., & Spivey, M. J. (2021). Is prediction nothing more than
1036 multi-scale pattern completion of the future? *Brain Research*, *1768*, 147578.
1037 <https://doi.org/10.1016/j.brainres.2021.147578>
- 1038 Federmeier, K. D. (2007). Thinking ahead: The role and roots of prediction in language
1039 comprehension. *Psychophysiology*, *44*(4), 491–505.
1040 <https://doi.org/10.1111/j.1469-8986.2007.00531.x>
- 1041 Feldman, H., & Friston, K. (2010). Attention, uncertainty, and free-energy. *Frontiers in*
1042 *Human Neuroscience*, *4*. <https://doi.org/10.3389/fnhum.2010.00215>

- 1043 Fitz, H., & Chang, F. (2019). Language ERPs reflect learning through prediction error
1044 propagation. *Cognitive Psychology*, *111*, 15–52.
1045 <https://doi.org/10.1016/j.cogpsych.2019.03.002>
- 1046 Fodor, J. (1983). Input systems as modules. In *The Modularity of Mind* (pp. 47–101). MIT
1047 Press.
- 1048 Forster, K. I. (1979). Levels of processing and the structure of the language processor. In
1049 W. Cooper & E. Walker (Eds.), *Sentence Processing: Psycholinguistic essays*
1050 *presented to Merrill Garrett* (pp. 27–85). Erlbaum.
- 1051 Friston, K. (2010). The free-energy principle: A unified brain theory? *Nature Reviews*
1052 *Neuroscience*, *11*(2), 127–138. <https://doi.org/10.1038/nrn2787>
- 1053 Gagl, B., Sassenhagen, J., Haan, S., Gregorova, K., Richlan, F., & Fiebach, C. J. (2020).
1054 An orthographic prediction error as the basis for efficient visual word recognition.
1055 *NeuroImage*, *214* (August 2019), 116727.
1056 <https://doi.org/10.1016/j.neuroimage.2020.116727>
- 1057 Gagnepain, P., Henson, R. N., & Davis, M. H. (2012). Temporal predictive codes for
1058 spoken words in auditory cortex. *Current Biology*, *22*(7), 615–621.
1059 <https://doi.org/10.1016/j.cub.2012.02.015>
- 1060 Getz, L. M., & Toscano, J. C. (2019). Electrophysiological evidence for top-down lexical
1061 influences on early speech perception. *Psychological Science*, *30*(6), 830–841.
1062 <https://doi.org/10.1177/0956797619841813>
- 1063 Groppe, D. M., Makeig, S., & Kutas, M. (2009). Identifying reliable independent
1064 components via split-half comparisons. *NeuroImage*, *45*(4), 1199–1211.
1065 <https://doi.org/10.1016/j.neuroimage.2008.12.038>
- 1066 Hauk, O., Coutout, C., Holden, A., & Chen, Y. (2012). The time-course of single-word
1067 reading: Evidence from fast behavioral and brain responses. *NeuroImage*, *60*(2),
1068 1462–1477. <https://doi.org/10.1016/j.neuroimage.2012.01.061>

- 1069 Huang, Z., Yang, S., Xue, L., Yang, H., Lv, Y., & Zhao, J. (2022). Level of orthographic
1070 knowledge helps to reveal automatic predictions in visual word processing. *Frontiers*
1071 *in Neuroscience*, *15*. <https://doi.org/10.3389/fnins.2021.809574>
- 1072 Hyvärinen, A., & Oja, E. (1997). A fast fixed-point algorithm for independent component
1073 analysis. *Neural Computation*, *9*(7), 1483–1492.
1074 <https://doi.org/10.1162/neco.1997.9.7.1483>
- 1075 Kanai, R., Komura, Y., Shipp, S., & Friston, K. (2015). Cerebral hierarchies: Predictive
1076 processing, precision and the pulvinar. *Philosophical Transactions of the Royal*
1077 *Society B: Biological Sciences*, *370*(1668). <https://doi.org/10.1098/rstb.2014.0169>
- 1078 Keuleers, E., Lacey, P., Rastle, K., & Brysbaert, M. (2012). The British Lexicon Project:
1079 Lexical decision data for 28,730 monosyllabic and disyllabic English words. *Behavior*
1080 *Research Methods*, *44*(1), 287–304. <https://doi.org/10.3758/s13428-011-0118-4>
- 1081 Kherif, F., Josse, G., & Price, C. J. (2011). Automatic top-down processing explains
1082 common left occipito-temporal responses to visual words and objects. *Cerebral*
1083 *Cortex*, *21*, 103–114. <https://doi.org/10.1093/cercor/bhq063>
- 1084 Kim, A., & Lai, V. (2012). Rapid interactions between lexical semantic and word form
1085 analysis during word recognition in context: Evidence from ERPs. *Journal of*
1086 *Cognitive Neuroscience*, *24*(5), 1104–1112. https://doi.org/10.1162/jocn_a_00148
- 1087 Kim, A. E., & Gilley, P. M. (2013). Neural mechanisms of rapid sensitivity to syntactic
1088 anomaly. *Frontiers in Psychology*, *4*, 1–15. <https://doi.org/10.3389/fpsyg.2013.00045>
- 1089 Kretschmar, F., Schlesewsky, M., & Staub, A. (2015). Dissociating word frequency and
1090 predictability effects in reading: Evidence from coregistration of eye movements and
1091 EEG. *Journal of Experimental Psychology : Learning, Memory, and Cognition*,
1092 *41*(6), 1648–1662. <https://doi.org/10.1037/xlm0000128>
- 1093 Kuperberg, G. R., & Jaeger, T. F. (2016). What do we mean by prediction in language
1094 comprehension? *Language, Cognition and Neuroscience*, *31*(1), 32–59.
1095 <https://doi.org/10.1080/23273798.2015.1102299>

- 1096 Kuperman, V., Stadthagen-Gonzalez, H., & Brysbaert, M. (2012). Age-of-acquisition
1097 ratings for 30,000 English words. *Behavior Research Methods*, *44*(4), 978–990.
1098 <https://doi.org/10.3758/s13428-012-0210-4>
- 1099 Kutas, M., & Federmeier, K. D. (2011). Thirty years and counting: Finding meaning in the
1100 N400 component of the event related brain potential (ERP). *Annual review of*
1101 *psychology*, *62*, 621–647. <https://doi.org/10.1146/annurev.psych.093008.131123>
- 1102 Kutas, M., & Hillyard, S. A. (1980). Reading senseless sentences: Brain potentials reflect
1103 semantic incongruity. *Science*, *207*, 203–205.
1104 <https://doi.org/10.1126/science.7350657>
- 1105 Lau, E. F., Holcomb, P. J., & Kuperberg, G. R. (2013). Dissociating N400 effects of
1106 prediction from association in single-word contexts. *Journal of Cognitive*
1107 *Neuroscience*, *25*(3), 484–502. https://doi.org/10.1162/jocn_a_00328
- 1108 Lin, S. E., Chen, H. C., Zhao, J., Li, S., He, S., & Weng, X. C. (2011). Left-lateralized
1109 N170 response to unpronounceable pseudo but not false Chinese characters - the key
1110 role of orthography. *Neuroscience*, *190*, 200–206.
1111 <https://doi.org/10.1016/j.neuroscience.2011.05.071>
- 1112 Lindborg, A., Musiolek, L., Ostwald, D., & Rabovsky, M. (2023). Semantic surprise
1113 predicts the N400 brain potential. *Neuroimage: Reports*, *3*(1), 100161.
1114 <https://doi.org/10.1016/j.ynirp.2023.100161>
- 1115 Ling, S., Lee, A. C. H., Armstrong, B. C., & Nestor, A. (2019). How are visual words
1116 represented? Insights from EEG-based visual word decoding, feature derivation and
1117 image reconstruction. *Human Brain Mapping*, *40*(17), 5056–5068.
1118 <https://doi.org/10.1002/hbm.24757>
- 1119 Luke, S. G., & Christianson, K. (2016). Limits on lexical prediction during reading.
1120 *Cognitive Psychology*, *88*, 22–60. <https://doi.org/10.1016/j.cogpsych.2016.06.002>
- 1121 Luthra, S., Li, M. Y. C., You, H., Brodbeck, C., & Magnuson, J. S. (2021). Does signal
1122 reduction imply predictive coding in models of spoken word recognition?

- 1123 *Psychonomic Bulletin & Review*, 28(4), 1381–1389.
1124 <https://doi.org/10.3758/s13423-021-01924-x>
- 1125 Mantegna, F., Hintz, F., Ostarek, M., Alday, P. M., & Huettig, F. (2019). Distinguishing
1126 integration and prediction accounts of ERP N400 modulations in language
1127 processing through experimental design. *Neuropsychologia*, 134, 107199.
1128 <https://doi.org/10.1016/j.neuropsychologia.2019.107199>
- 1129 MATLAB. (2022). *MATLAB Version 9.13.0 (R2022b)*. The MathWorks Inc.
- 1130 Maurer, U., Brandeis, D., & McCandliss, B. D. (2005). Fast, visual specialization for
1131 reading in English revealed by the topography of the N170 ERP response.
1132 *Behavioral and Brain Functions*, 1, 1–12. <https://doi.org/10.1186/1744-9081-1-13>
- 1133 Maurer, U., Brem, S., Bucher, K., & Brandeis, D. (2005). Emerging neurophysiological
1134 specialization for letter strings. *Journal of Cognitive Neuroscience*, 17(10),
1135 1532–1552. <https://doi.org/10.1162/089892905774597218>
- 1136 Maurer, U., Rossion, B., & McCandliss, B. D. (2008). Category specificity in early
1137 perception: Face and word N170 responses differ in both lateralization and
1138 habituation properties. *Frontiers in Human Neuroscience*, 2, 1–7.
1139 <https://doi.org/10.3389/neuro.09.018.2008>
- 1140 McClelland, J. L., & Rumelhart, D. E. (1981). An interactive activation model of context
1141 effects in letter perception: Part 1. An account of basic findings. *Psychological*
1142 *Review*, 88(5), 375–407. <https://doi.org/10.1037/0033-295X.88.5.375>
- 1143 Nieuwland, M. S. (2019). Do 'early' brain responses reveal word form prediction during
1144 language comprehension? A critical review. *Neuroscience and Biobehavioral*
1145 *Reviews*, 96, 367–400. <https://doi.org/10.1016/j.neubiorev.2018.11.019>
- 1146 Nobre, A. C., Allison, T., & McCarthy, G. (1994). Word recognition in the human inferior
1147 temporal lobe. *372*, 260–263. <https://doi.org/10.1038/372260a0>

- 1148 Pastore, M., & Calcagni, A. (2019). Measuring distribution similarities between samples: A
1149 distribution-free overlapping index. *Frontiers in Psychology*, *10*(1089), 1–8.
1150 <https://doi.org/10.3389/fpsyg.2019.01089>
- 1151 Peirce, J. W. (2007). PsychoPy - Psychophysics software in Python. *Journal of*
1152 *Neuroscience Methods*, *162*(1-2), 8–13.
1153 <https://doi.org/10.1016/j.jneumeth.2006.11.017>
- 1154 Penolazzi, B., Hauk, O., & Pulvermüller, F. (2007). Early semantic context integration and
1155 lexical access as revealed by event-related brain potentials. *Biological Psychology*,
1156 *74*(3), 374–388. <https://doi.org/10.1016/j.biopsycho.2006.09.008>
- 1157 Pickering, M. J., & Gambi, C. (2018). Predicting while comprehending language: A theory
1158 and review. *Psychological Bulletin*, *144*(10), 1002–1044.
1159 <https://doi.org/10.1037/bul0000158>
- 1160 Pickering, M. J., & Garrod, S. (2013). An integrated theory of language production and
1161 comprehension. *Behavioral and Brain Sciences*, *36*(4), 329–347.
1162 <https://doi.org/10.1017/S0140525X12001495>
- 1163 Pion-Tonachini, L., Kreutz-Delgado, K., & Makeig, S. (2019). ICLabel: An automated
1164 electroencephalographic independent component classifier, dataset, and website.
1165 *NeuroImage*, *198*, 181–197. <https://doi.org/10.1016/j.neuroimage.2019.05.026>
- 1166 Pleisch, G., Karipidis, I. I., Brem, A., Röthlisberger, M., Roth, A., Brandeis, D.,
1167 Walitza, S., & Brem, S. (2019). Simultaneous EEG and fMRI reveals stronger
1168 sensitivity to orthographic strings in the left occipito-temporal cortex of typical
1169 versus poor beginning readers. *Developmental Cognitive Neuroscience*, *40*, 1–13.
1170 <https://doi.org/10.1016/j.dcn.2019.100717>
- 1171 Powell, M. (2009). The BOBYQA algorithm for bound constrained optimization without
1172 derivatives. *Cambridge NA Report NA2009/06*, University of Cambridge,
1173 Cambridge, 26–46. <https://doi.org/10.1.1.443.7693>

- 1174 Price, C. J., & Devlin, J. T. (2011). The Interactive Account of ventral occipitotemporal
1175 contributions to reading. *Trends in Cognitive Sciences*, 15(6), 246–253.
1176 <https://doi.org/10.1016/j.tics.2011.04.001>
- 1177 R Core Team. (2021). *R: A language and environment for statistical computing*. R
1178 Foundation for Statistical Computing. <https://www.r-project.org/>
- 1179 Rabovsky, M., & McRae, K. (2014). Simulating the N400 ERP component as semantic
1180 network error: Insights from a feature-based connectionist attractor model of word
1181 meaning. *Cognition*, 132(1), 68–89. <https://doi.org/10.1016/j.cognition.2014.03.010>
- 1182 Rao, R. P., & Ballard, D. H. (1999). Predictive coding in the visual cortex: A functional
1183 interpretation of some extra-classical receptive-field effects. *Nature Neuroscience*,
1184 2(1), 79–87. <https://doi.org/10.1038/4580>
- 1185 Rauschecker, A. M., Bowen, R. F., Parvizi, J., & Wandell, B. A. (2012). Position sensitivity
1186 in the visual word form area. *Proceedings of the National Academy of Sciences of
1187 the United States of America*, 109(24). <https://doi.org/10.1073/pnas.1121304109>
- 1188 Rauss, K., Schwartz, S., & Pourtois, G. (2011). Top-down effects on early visual processing
1189 in humans: A predictive coding framework [Publisher: Elsevier Ltd]. *Neuroscience
1190 and Biobehavioral Reviews*, 35(5), 1237–1253.
1191 <https://doi.org/10.1016/j.neubiorev.2010.12.011>
- 1192 Rayner, K., Slattery, T. J., Drieghe, D., & Liversedge, S. P. (2011). Eye movements and
1193 word skipping during reading: Effects of word length and predictability. *Journal of
1194 Experimental Psychology: Human Perception and Performance*, 37, 514–528.
1195 <https://doi.org/10.1037/a0020990>
- 1196 Rodrigues, A. P., Rebola, J., Pereira, M., Van Asselen, M., & Castelo-Branco, M. (2019).
1197 Neural responses of the anterior ventral occipitotemporal cortex in developmental
1198 dyslexia: Beyond the visual word form area. *Investigative Ophthalmology and Visual
1199 Science*, 60(4), 1063–1068. <https://doi.org/10.1167/iovs.18-26325>

- 1200 Rousselet, G. A. (2012). Does filtering preclude us from studying ERP time-courses?
1201 *Frontiers in Psychology, 3*, 1–9. <https://doi.org/10.3389/fpsyg.2012.00131>
- 1202 Schuster, S., Himmelstoss, N. A., Hutzler, F., Richlan, F., Kronbichler, M., & Hawelka, S.
1203 (2021). Cloze enough? Hemodynamic effects of predictive processing during natural
1204 reading. *NeuroImage, 228*, 117687.
1205 <https://doi.org/10.1016/j.neuroimage.2020.117687>
- 1206 Segalowitz, S. J., & Zheng, X. (2009). An ERP study of category priming: Evidence of
1207 early lexical semantic access. *Biological Psychology, 80*(1), 122–129.
1208 <https://doi.org/10.1016/j.biopsycho.2008.04.009>
- 1209 Sereno, S. C., Brewer, C. C., & O'Donnell, P. J. (2003). Context effects in word
1210 recognition: Evidence for early interactive processing. *Psychological Science, 14*(4),
1211 328–333. <https://doi.org/10.1111/1467-9280.14471>
- 1212 Sereno, S. C., Hand, C. J., Shahid, A., Mackenzie, I. G., & Leuthold, H. (2019). Early EEG
1213 correlates of word frequency and contextual predictability in reading [Publisher:
1214 Taylor & Francis]. *Language, Cognition and Neuroscience, 35*(5), 625–640.
1215 <https://doi.org/10.1080/23273798.2019.1580753>
- 1216 Sereno, S. C., Rayner, K., & Posner, M. I. (1998). Establishing a time-line of word
1217 recognition: Evidence from eye movements and event-related potentials.
1218 *NeuroReport, 9*(10), 2195–2200. <https://doi.org/10.1097/00001756-199807130-00009>
- 1219 Shain, C., Blank, I. A., van Schijndel, M., Schuler, W., & Fedorenko, E. (2020). fMRI
1220 reveals language-specific predictive coding during naturalistic sentence
1221 comprehension. *Neuropsychologia, 138*, 107307.
1222 <https://doi.org/10.1016/j.neuropsychologia.2019.107307>
- 1223 Sperber, R. D., McCauley, C., Ragain, R. D., & Weil, C. M. (1979). Semantic priming
1224 effects on picture and word processing. *Memory & Cognition, 7*(5), 339–345.
1225 <https://doi.org/10.3758/BF03196937>

- 1226 STAN Development Team. (2023). Stan Modeling Language Users Guide and Reference
1227 Manual, 2.32. <https://mc-stan.org>
- 1228 Strijkers, K., Bertrand, D., & Grainger, J. (2015). Seeing the same words differently: The
1229 time course of automaticity and top-down intention in reading. *Journal of Cognitive*
1230 *Neuroscience*, *27*(8), 1542–1551. https://doi.org/10.1162/jocn_a_00797
- 1231 Taha, H., Ibrahim, R., & Khateb, A. (2013). How does arabic orthographic connectivity
1232 modulate brain activity during visual word recognition: An ERP study. *Brain*
1233 *Topography*, *26*(2), 292–302. <https://doi.org/10.1007/s10548-012-0241-2>
- 1234 Tanner, D., Morgan-Short, K., & Luck, S. J. (2015). How inappropriate high-pass filters can
1235 produce artifactual effects and incorrect conclusions in ERP studies of language and
1236 cognition. *Psychophysiology*, *52*(8), 997–1009. <https://doi.org/10.1111/psyp.12437>
- 1237 Taylor, J. E., Beith, A., & Sereno, S. C. (2020). LexOPS: An R package and user interface
1238 for the controlled generation of word stimuli. *Behavior Research Methods*, *52*,
1239 *2372–2382*. <https://doi.org/10.3758/s13428-020-01389-1>
- 1240 Thaler, L., Schütz, A. C., Goodale, M. A., & Gegenfurtner, K. R. (2013). What is the best
1241 fixation target? The effect of target shape on stability of fixational eye movements.
1242 *Vision Research*, *76*, 31–42. <https://doi.org/10.1016/j.visres.2012.10.012>
- 1243 Tsogli, V., Jentschke, S., & Koelsch, S. (2022). Unpredictability of the “when” influences
1244 prediction error processing of the “what” and “where” [Publisher: Public Library of
1245 Science]. *PLOS ONE*, *17*(2), e0263373.
1246 <https://doi.org/10.1371/journal.pone.0263373>
- 1247 Van Petten, C., & Kutas, M. (1990). Interactions between sentence context and word
1248 frequency in event-related brain potentials. *Memory & Cognition*, *18*(4), 380–393.
1249 <https://doi.org/10.3758/BF03197127>
- 1250 Van Petten, C., & Luka, B. J. (2012). Prediction during language comprehension: Benefits,
1251 costs, and ERP components. *International Journal of Psychophysiology*, *83*(2),
1252 *176–190*. <https://doi.org/10.1016/j.ijpsycho.2011.09.015>

- 1253 Vanderwart, M. (1984). Priming by pictures in lexical decision. *Journal of Verbal Learning*
1254 *and Verbal Behavior*, 23(1), 67–83. [https://doi.org/10.1016/S0022-5371\(84\)90509-7](https://doi.org/10.1016/S0022-5371(84)90509-7)
- 1255 van Heuven, W. J., Mandera, P., Keuleers, E., & Brysbaert, M. (2014). SUBTLEX-UK: A
1256 new and improved word frequency database for British English. *Quarterly Journal*
1257 *of Experimental Psychology*, 67(6), 1176–1190.
1258 <https://doi.org/10.1080/17470218.2013.850521>
- 1259 VanRullen, R. (2011). Four common conceptual fallacies in mapping the time course of
1260 recognition. *Frontiers in Psychology*, 2, 1–6.
1261 <https://doi.org/10.3389/fpsyg.2011.00365>
- 1262 Veale, J. F. (2014). Edinburgh Handedness Inventory - Short Form: A revised version based
1263 on confirmatory factor analysis. *Laterality*, 19(2), 164–177.
1264 <https://doi.org/10.1080/1357650X.2013.783045>
- 1265 Vidal, C., Content, A., & Chetail, F. (2017). BACS: The Brussels Artificial Character Sets
1266 for studies in cognitive psychology and neuroscience. *Behavior Research Methods*,
1267 49(6), 2093–2112. <https://doi.org/10.3758/s13428-016-0844-8>
- 1268 Walsh, K. S., McGovern, D. P., Clark, A., & O’Connell, R. G. (2020). Evaluating the
1269 neurophysiological evidence for predictive processing as a model of perception.
1270 *Annals of the New York Academy of Sciences*, 1464(1), 242–268.
1271 <https://doi.org/10.1111/nyas.14321>
- 1272 Wang, F., & Maurer, U. (2017). Top-down modulation of early print-tuned neural activity
1273 in reading. *Neuropsychologia*, 102, 29–38.
1274 <https://doi.org/10.1016/j.neuropsychologia.2017.05.028>
- 1275 Wang, F., & Maurer, U. (2020). Interaction of top-down category-level expectation and
1276 bottom-up sensory input in early stages of visual-orthographic processing.
1277 *Neuropsychologia*, 137, 107299.
1278 <https://doi.org/10.1016/j.neuropsychologia.2019.107299>

- 1279 Warriner, A. B., Kuperman, V., & Brysbaert, M. (2013). Norms of valence, arousal, and
1280 dominance for 13,915 English lemmas. *Behavior Research Methods*, *45*(4),
1281 1191–1207. <https://doi.org/10.3758/s13428-012-0314-x>
- 1282 White, A. L., Palmer, J., Boynton, G. M., & Yeatman, J. D. (2019). Parallel spatial
1283 channels converge at a bottleneck in anterior word-selective cortex. *Proceedings of*
1284 *the National Academy of Sciences of the United States of America*, *116*(20),
1285 10087–10096. <https://doi.org/10.1073/pnas.1822137116>
- 1286 Woolnough, O., Donos, C., Rollo, P. S., Forseth, K. J., Lakretz, Y., Crone, N. E.,
1287 Fischer-Baum, S., Dehaene, S., & Tandon, N. (2021). Spatiotemporal dynamics of
1288 orthographic and lexical processing in the ventral visual pathway. *Nature Human*
1289 *Behaviour*, *5*(3), 389–398. <https://doi.org/10.1038/s41562-020-00982-w>
- 1290 Yarkoni, T., Balota, D., & Yap, M. (2008). Moving beyond Coltheart’s N: A new measure
1291 of orthographic similarity. *Psychonomic Bulletin and Review*, *15*(5), 971–979.
1292 <https://doi.org/10.3758/PBR.15.5.971>
- 1293 Yeatman, J. D., Rauschecker, A. M., & Wandell, B. A. (2013). Anatomy of the visual word
1294 form area: Adjacent cortical circuits and long-range white matter connections. *Brain*
1295 *and Language*, *125*(2), 146–155. <https://doi.org/10.1016/j.bandl.2012.04.010>
- 1296 Ylinen, S., Bosseler, A., Junntila, K., & Huotilainen, M. (2017). Predictive coding
1297 accelerates word recognition and learning in the early stages of language
1298 development. *Developmental Science*, *20*(6), e12472.
1299 <https://doi.org/10.1111/desc.12472>
- 1300 Ylinen, S., Huuskonen, M., Mikkola, K., Saure, E., Sinkkonen, T., & Paavilainen, P. (2016).
1301 Predictive coding of phonological rules in auditory cortex: A mismatch negativity
1302 study. *Brain and Language*, *162*, 72–80. <https://doi.org/10.1016/j.bandl.2016.08.007>
- 1303 Zhao, J., Kipp, K., Gaspar, C., Maurer, U., Weng, X., Mecklinger, A., & Li, S. (2014). Fine
1304 neural tuning for orthographic properties of words emerges early in children reading

- 1305 alphabetic script. *Journal of Cognitive Neuroscience*, *26*(11), 2431–2442.
1306 https://doi.org/10.1162/jocn_a_00660
- 1307 Zhao, J., Maurer, U., He, S., & Weng, X. (2019). Development of neural specialization for
1308 print: Evidence for predictive coding in visual word recognition. *PLoS Biology*,
1309 *17*(10), 1–17. <https://doi.org/10.1371/journal.pbio.3000474>